

AD-A009 716

ANALYSIS OF FLOW AND HEAT TRANSFER IN SMALL ARMS

Edward V. McAssey, Jr.

Villanova University

Prepared for:

Army Research Office
Frankford Arsenal

1 April 1975

DISTRIBUTED BY:

NTIS

National Technical Information Service
U. S. DEPARTMENT OF COMMERCE

Unclassified

SECURITY CLASSIFICATION OF THIS PAGE (When Data Entered)

REPORT DOCUMENTATION PAGE		READ INSTRUCTIONS BEFORE COMPLETING FORM	
1. REPORT NUMBER Project #286	2. GOVT ACCESSION NO.	3. RECIPIENT'S CATALOG NUMBER AD-A009 716	
4. TITLE (and Subtitle) Analysis of Flow and Heat Transfer in Small Arms		5. TYPE OF REPORT & PERIOD COVERED Final 1 Nov. 73 to 1 April 75	
		6. PERFORMING ORG. REPORT NUMBER	
7. AUTHOR(s) Edward V. McAssey, Jr.		8. CONTRACT OR GRANT NUMBER(s) DAHC04-74-G-0044	
9. PERFORMING ORGANIZATION NAME AND ADDRESS Mechanical Engineering Department Villanova, University, Villanova, Pa. 19085		10. PROGRAM ELEMENT, PROJECT, TASK AREA & WORK UNIT NUMBERS P-12080-RTL	
11. CONTROLLING OFFICE NAME AND ADDRESS U. S. Army Research Office Box CM, Duke Station Durham, North Carolina 27706		12. REPORT DATE 1 April 1975	
		13. NUMBER OF PAGES 25	
14. MONITORING AGENCY NAME & ADDRESS (if different from Controlling Office) Frankford Arsenal Bridge & Tacony St. Philadelphia, Pa. 19137		15. SECURITY CLASS. (of this report) Unclassified	
		16a. DECLASSIFICATION/DOWNGRADING SCHEDULE NA	
16. DISTRIBUTION STATEMENT (of this Report) Approved for public release; distribution unlimited.			
17. DISTRIBUTION STATEMENT (of the abstract entered in Block 20, if different from Report) NA			
18. SUPPLEMENTARY NOTES			
19. KEY WORDS (Continue on reverse side if necessary and identify by block number) Transient Flow, Heat Transfer, Flow in Small Arms, Flame Front			
20. ABSTRACT (Continue on reverse side if necessary and identify by block number) A computer model of the pressure distribution and flow characteristics in small arms barrels has been developed. This model shows the sensitivity of the pressure history and launch velocity of surface concentration density of deterrent, flame front velocity, and projectile base heating.			

Reproduced by
NATIONAL TECHNICAL
INFORMATION SERVICE
US Department of Commerce
Springfield, VA. 22151

PRICES SUBJECT TO CHANGE

DD FORM 1 JAN 73 1473

EDITION OF 1 NOV 65 IS OBSOLETE

Unclassified

SECURITY CLASSIFICATION OF THIS PAGE (When Data Entered)

ANALYSIS OF FLOW AND HEAT TRANSFER
IN SMALL ARMS

Edward V. McAssèy, Jr.

April 1, 1975

Sponsored by U.S. Army Research Office
Durham, N. C., Grant DAHC04-74-G-0044
Project No. 286

Mechanical Engineering Department
Villanova University

Approved for Public Release;
Distribution Unlimited

Abstract

A computer model of the pressure distribution and flow characteristics in small arms barrels has been developed. This model shows the sensitivity of the pressure history and launch velocity to surface concentration density of deterrent, flame front velocity, and projectile base heating.

ALL FINDINGS IN THIS REPORT ARE NOT TO BE CONSTRUED AS AN OFFICIAL DEPARTMENT OF THE ARMY POSITION, UNLESS SO DESIGNATED BY OTHER AUTHORIZED DOCUMENTS.

TABLE OF CONTENTS

	Page No.
Abstract	1
Nomenclature	3
Introduction	5
Literature Review	7
Analysis	10
Numerical Results	37
Conclusions and Recommendations	47
References	48
Appendix A	
Appendix B	

NOMENCLATURE

- A cross-sectional area of gun bore, ft^2
- a speed of sound, ft/sec
- c_p specific heat of propellant gas at constant pressure, $BTU/lbm-^{\circ}R$
- c_v specific heat of propellant gas at constant volume, $BTU/lbm-^{\circ}R$
- D diameter of gun bore, ft
- D_0 initial diameter of propellant grain (weighted average), ft
- E_{gas} energy per unit mass of gas, $BTU/slug$
- F_d drag force on propellant particles per unit volume, lbf/ft^3
- g acceleration of gravity, ft/sec^2
- H enthalpy, $BTU/slug$
- J mechanical equivalent of heat, $ft-lbf/BTU$
- z distance burned normal to propellant grain surface, ft
- m_g rate of mass of gas generated per unit length, $slug/ft-sec$
- p gas pressure, lbf/ft^2
- q heat loss through barrel wall, BTU/ft^2-sec
- R gas constant for propellant gas, $ft-lbf/slug-^{\circ}R$
- \bar{R} disk radius for an individual grain, ft
- R_i one half of web thickness of individual grain, ft
- r linear burning rate of propellant, ft/sec
- s specific entropy, $BTU/lbm-^{\circ}R$
- S_p surface area of an individual grain, ft^2
- T_g gas temperature, $^{\circ}R$
- t time, sec
- u_g velocity of gas, ft/sec
- u_p velocity of propellant particles, ft/sec

V_p	volume of an individual grain, ft^3
W	powder potential, $\text{cvT}(\ell)$, BTU/lbm
W_t	weight of projectile, lbm
ϵ	particle volume fraction, dimensionless
η	number of particle grains per unit volume, ft^{-3}
ρ_g	gas density, slug/ ft^3
ρ_p	propellant density, slug/ ft^3
τ_w	wall shearing stress, lbf/ft^2 or slug/ $\text{ft}\text{-sec}^2$

Introduction

Investigations into propellant performance, barrel materials and weapon kinematics require accurate description of the weapon interior ballistics. The present study was undertaken to determine the effect of heat transfer on interior ballistics. In examining the interior ballistics of small arms, the effect of a number of parameters must be included. These parameters include chamber geometry, propellant geometry, propellant composition and burning rate.

The heat transfer rates in small arms are very high and are considered to be a major cause of barrel erosion. Accurate description of these heat transfer rates is necessary for analytical predication of pressure and velocity histories in small arms.

The present study uses the method of characteristics to solve the governing equations. The model assumes the problem to be one dimensional and transient. Assuming a fixed propellant description, the effect of various heat transfer models has been examined. The performance standard is test data from reference 1 presented in figure 1.

PRESSURE & VELOCITY VS. TRAVEL

EXPERIMENTAL DATA REF 1

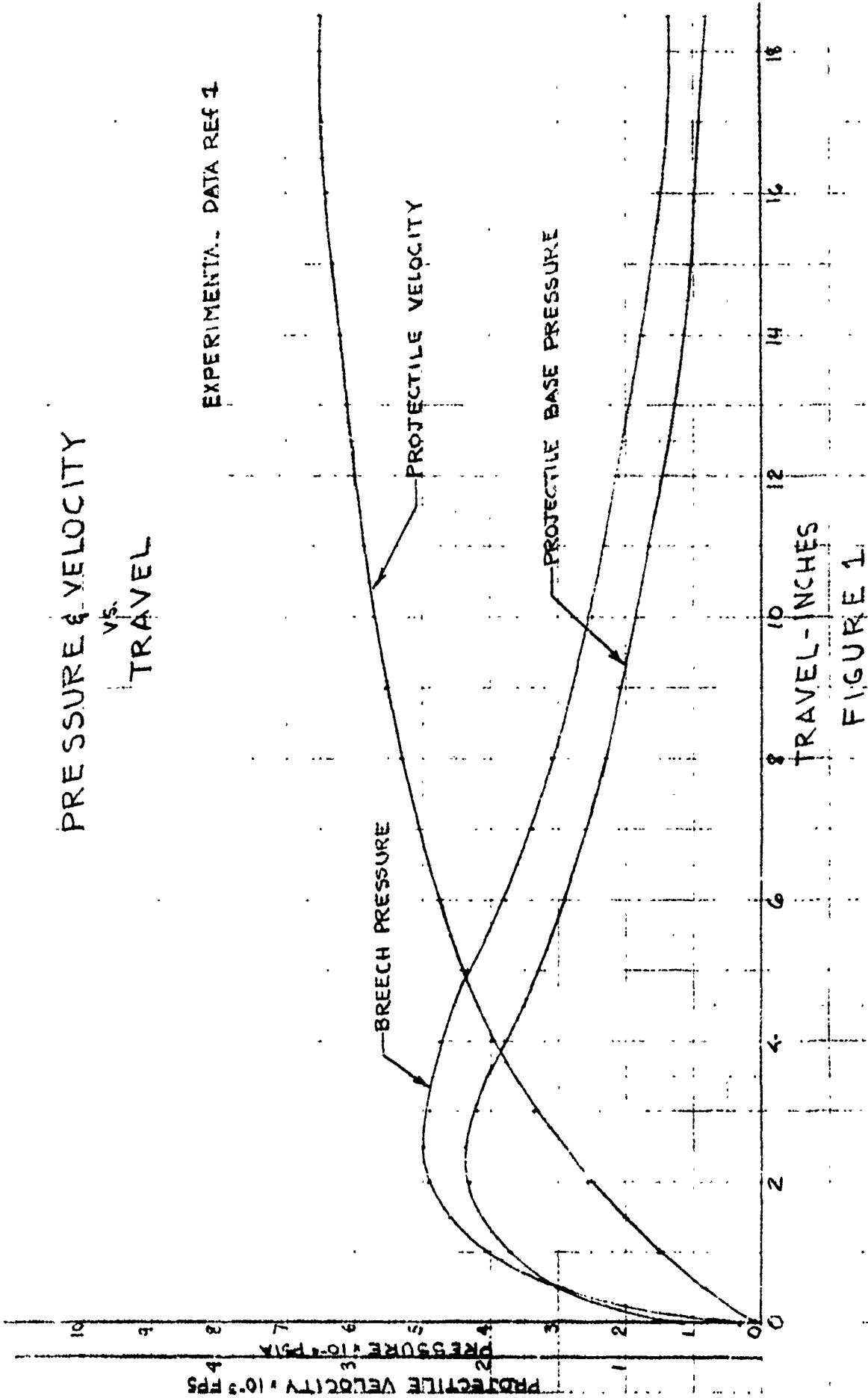


FIGURE 1

Literature Survey

Reference (2) presents a ballistic model developed from earlier work which was modified to include the effect of non-uniform propellant composition and non-simultaneous ignition. In this reference the propellant is represented by a composite of 9 different composition propellants. This variable propellant array allows the handling of different size grains and different deterrent concentration densities. Sample results are included in reference (2) which shows good agreement with test.

Reference (3) presents an analytical investigation of the flow in gun barrels with particular emphasis on the heat transfer. In addition to the transient nature of the flow, reference (3) considers the problem posed by the lack of a boundary layer at the base of the projectile. This condition occurs because in the projectile based region the gas velocity is equal to the projectile velocity. This condition means that the Reynolds analogy commonly used in heat transfer cannot be applied to this case. However, the reference does propose an expression for heat transfer coefficient in the projectile base region. The resulting convective coefficients are between 5 and 20 Btu/sec ft² °F. Comparisons between experiment and prediction presented in reference (3) indicate that even these high coefficients underestimate the actual results. However, the results of reference (3) represent the best available procedure for calculating the heating at the base of the projectile.

Reference (4) presented an analytical study of interior ballistics in which the governing equations were solved using a finite difference procedure. The geometric dimensions used in reference (4) did not correspond to standard small arms. In addition, the analysis was limited to stationary propellant and to propellant moving at the same velocity as the gas. In the area of heat transfer reference (4) also obtained very high heat transfer coefficients

(~ 10 Btu/sec ft² °F). It is worthy of note that for cases with and without heat transfer and wall friction the ballistic performance was not changed significantly. The present study has found that heat transfer particularly at the projectile base, is very significant.

Reference (5) presents an extensive study of the flame front movement through a porous bed propellant. The analysis is presented for a venting bomb type device. However, the results for flame propagation can be applied to the small arms case. Indeed, the functional relationship between flame velocity and pressure can be obtained from the data presented in reference (5). Reference (6) considers the same problem as reference (5) but applied to the small arms case. The results of reference (6) have been used in the present study to determine the progress of the flame front through the propellant bed. Reference (7) presents an iterative model for the interior ballistic problem in which parameters affecting the burning rate were changed until the calculated results agreed with test data. The caliber used in reference (7) is the same as the present study, (i.e. 5.56 MM); however, the experimental and analytical results are considerably different. This is most likely due to different charge weight and propellant type. In addition, a number of the loss factors considered in the present study are not included.

Reference (8) is the analytical basis for the present study. This reference presents the model which has been used and also outlines the calculation procedure for the method of characteristics. The nomenclature of reference (8) has been adopted in the present report. The present investigation has expended considerable effort in programming reference (8). Reference (8) describes the interior ballistic problem as a one dimensional transient flow problem. In the model the propellant is assumed to ignite instantaneously and burn at a rate proportional to the gas pressure. The geometry of the propellant is uniform and based upon reference (10).

Although heat transfer between the gas and propellant is neglected, drag between these two is considered. The transformation of the governing equations from the physical domain to the characteristic domain is described in detail in reference (9). The heat transfer to the wall and the wall friction are included in the model but the detailed descriptions are developed in the present study. In addition, the effect of chamberage and projectile resistive forces are also included in the model of reference (9).

Analysis

To determine the effect of heat transfer and to evaluate potential heat transfer relationships, an accurate model of the flow field must be developed. Considerable effort during the present study was devoted to developing a model which could reproduce test data. In addition, during the course of this model development it became apparent that the assumption of uniform ignition was not adequate and therefore a more realistic flame front model had to be developed. This section describes the flow field flame front analysis, and heat transfer models.

The flow is two phase, non-steady, including heat and mass addition. The basic model describing the problem has been developed in reference (8). Because of the geometry present, the problem is quasi-one dimensional. The resulting conservation equations form a set of quasi-linear partial differential equations of the first order and hyperbolic type. For this situation the method of characteristics provides the simplest means of solution. Reference (8) provides the details of the transformation of the governing equations to the characteristic form. In addition, reference (9) provides the theoretical foundation for the applications of the method of characteristic to the present problem.

Flow Field Governing Equations

The governing equations described in these sections are based upon the following assumptions:

1. Flow is quasi-one dimensional
2. The gas is assumed to be ideal
3. The specific heat and molecular weight are dependent upon the amount of detherred and non-detherred propellant burned
4. All propellants grains are initially of uniform surface area, volume, and radius. Weighted mean values based upon reference (10) and (11) are used.
5. Interactions between individual propellant particles and between particles and the boundary are negligible
6. The thermal motion of the propellant particles does not contribute to the pressure
7. The average gas temperature is defined by the heat content of the gas phase
8. The propellant particles are spheres for drag calculations
9. Heat dissipation due to viscosity is negligible
10. Radiation is negligible
11. Gravity is negligible

$$\frac{\partial}{\partial t} (\rho_g A (1-\epsilon)) + \frac{\partial}{\partial x} (\rho_g A U_g (1-\epsilon)) = \dot{m}_g \quad (1)$$

where \dot{m}_g is the gas generated per unit length

$$\dot{m}_g = \epsilon S_p r \rho_p A / V_p$$

Propellant Particle Continuity Equation

$$\frac{D\epsilon}{Dt} = -\epsilon \frac{\partial U_p}{\partial x} - \frac{\epsilon U_p}{A} \frac{\partial A}{\partial x} - \frac{\dot{m}_g}{A \rho_p} \quad (2)$$

Overall Gas Momentum Equation

$$\begin{aligned} A \rho_g (1-\epsilon) \frac{\partial U_g}{\partial t} + (1-\epsilon) U_g \rho_g A \frac{\partial U_g}{\partial x} \\ = -U_g \dot{m}_g - \tau_w \pi D - (1-\epsilon) A \frac{\partial P}{\partial x} \\ - F_d A \end{aligned} \quad (3)$$

where τ_w is shear stress at the wall and F_d is particle drag per unit volume

Propellant Particle Momentum Equation

$$\frac{D U_p}{Dt} = \frac{U_p \dot{m}_g}{\rho_p A \epsilon} + \frac{F_d}{\rho_p \epsilon} \quad (4)$$

Overall Gas Energy Equation

$$\begin{aligned} \frac{\partial}{\partial t} ((1-\epsilon) \rho_g (\frac{U_g^2}{2} + g c_v T_g) A) \\ + \frac{\partial}{\partial x} ((1-\epsilon) \rho_g A U_g (g c_v T_g + \frac{P}{\rho_g} + \frac{U_g^2}{2})) \\ = -g \pi D - \frac{F_d A}{J} |U_g - U_p| + g W \dot{m}_g \end{aligned} \quad (5)$$

where W is the heat content of the propellant per pound

Overall Gas Entropy Equation

$$\frac{DS}{Dt} = (\bar{E}_{gas} + \frac{U_g F}{J} - R_s) / (A(1-\epsilon) \rho_g T_g g) \quad (6)$$

where.

$$E_{gas} = -g \pi D - \frac{F_d A |U_g - U_p|}{J} + g W \dot{m}_g$$

$$F = -U_g \dot{m}_g + \tau_w \pi D + F_d A$$

$$R_s = \dot{m}_g (g c_v T_g + \frac{U_g^2}{2J}) + \frac{PA}{J} \frac{\partial \epsilon}{\partial t} + \frac{P \dot{m}_g}{\rho_g J}$$

In the preceding equations, the dependent gas variables are entropy, gas temperature, pressure, gas density and gas velocity.

The next step in the solution procedure is to apply the method of characteristics. In this approach the dependent variables become the P and Q Riemann variables where:

$$P = \frac{2}{\gamma-1} a + U_g$$

$$Q = \frac{2}{\gamma-1} a - U_g$$

Solutions are determined along these P and Q characteristics. The characteristics represent lines along which infinitesimal disturbances are propagated at the local speed of sound in the gas phase. Along each characteristic the following relationships between X, t are true:

$$\frac{dx}{dt} = U_g + a \quad (\text{along P characteristic})$$

$$\frac{dx}{dt} = U_g - a \quad (\text{along Q characteristic})$$

Equation (1) and (3) can be combined into two equations for P and Q along the respective characteristic using the ideal gas relations (for details see reference (3)):

$$a^2 = \gamma R T_g$$

$$\ln P = \frac{\gamma}{\gamma-1} \ln a - g \frac{J S}{R}$$

yielding equations (7) and (8).

$$\begin{aligned}
 \frac{\delta \pm P}{\delta t} = & -a U_g \frac{\partial}{\partial x} \ln A + \frac{\gamma-1}{\gamma} \frac{a g J}{R} \frac{D S}{D t} \\
 & + \frac{a g J}{\gamma R} \frac{\delta \pm S}{\delta t} - \frac{\gamma_0 \pi D}{A(1-\epsilon) \rho_g} - a \frac{D}{D t} \ln(1-\epsilon) \\
 & - \frac{F_d}{\rho_g(1-\epsilon)} - \frac{U_g v_{ig}}{A(1-\epsilon) \rho_g} + \frac{a^3 v_{ig}}{A(1-\epsilon) P \gamma} \quad (7)
 \end{aligned}$$

$$\begin{aligned}
 \frac{\delta \pm Q}{\delta t} = & -a U_g \frac{\partial}{\partial x} \ln A + \frac{(\beta-1)}{\beta} \frac{a g J}{R} \frac{D S}{D t} \\
 & + \frac{a g J}{\gamma R} \frac{\delta \pm S}{\delta t} + \frac{\gamma_0 \pi D}{A(1-\epsilon) \rho_g} - a \frac{D}{D t} \ln(1-\epsilon) \\
 & + \frac{F_d}{\rho_g(1-\epsilon)} + \frac{U_g v_{ig}}{A(1-\epsilon) \rho_g} + \frac{a^3 v_{ig}}{A(1-\epsilon) P \gamma} \quad (8)
 \end{aligned}$$

where:

$$\frac{\delta \pm}{\delta t} = \frac{\partial}{\partial t} + (U_g \pm a) \frac{\partial}{\partial x}$$

Equation (6), (7) and (8) along with the appropriate ideal gas relations are the governing equations for the gas phase. Equations (2) and (4) describe the propellant particle phase.

Initial and Boundary Conditions

At $t=0$, the first Q wave leaves the base of the projectile and travels toward the breech. During the time prior to the arrival of the Q wave at the breech, it is assumed that the gas in the chamber is at rest and that the temperature is constant at the flame temperature, T_0 . The pressure in the region between the projectile and breech will rise as the Q wave advances

due to the burning of propellant. The slope of this first Q wave is given by equation (9).

$$\frac{dx}{dt} = -a_0 = -\sqrt{\gamma R T_0} \quad (9)$$

The Q wave is divided into a specified number of equally spaced nodes.

The nodes are the origin for the P wave. At each node the gas temperature and speed of sound are known, the other parameters are given by the following relations:

$$t_{i+1} = t_i + \frac{(x_{i+1} - x_i)}{a_0}$$

$$\frac{DS}{Dt} = \left(g_w \dot{m}_g - \dot{m}_g \left(g c_v T_g + \frac{P}{\rho_g J} \right) - \frac{P_A}{J} \frac{D\epsilon}{Dt} \right) / (A (1-\epsilon) \rho_g T_g)$$

$$\frac{D\epsilon}{Dt} = - \frac{\dot{m}_g}{A \rho_p}$$

$$S_{i+1} = S_i + \frac{DS}{Dt} (t_{i+1} - t_i)$$

$$P_{i+1} = P_i e^{-\frac{qT}{R} (S_{i+1} - S_i)}$$

Since the speed of sound is constant along this wave, Q is also constant. This procedure is different from that described in reference 8, but it yields the same results.

The spatial boundaries of the problem are the breech ($x=0$) and the base of the projectile. The breech is at a fixed condition with the gas and propellant velocity equal to zero. The location of the projectile base is determined by the intersection of a P wave and the equation of motion of the projectile. The two equations governing the position of the projectile are:

$$\frac{dx}{dt} = U_g + a \quad (10)$$

$$\frac{d^2x}{dt^2} = \frac{qAP}{W_t} - \frac{qR_1}{W_t} \quad (11)$$

where R_1 is the engraving force and W_t is the weight of the projectile.

At the projectile base the gas velocity, propellant velocity and projectile velocity are all equal.

Numerical Procedure

The numerical solutions to the governing equation will be obtained using the finite difference procedure. In this approach, derivatives will be replaced by finite differences (explicit) and these will be used to generate the desired characteristic grid. Fig 1 shows the proposed grid system.

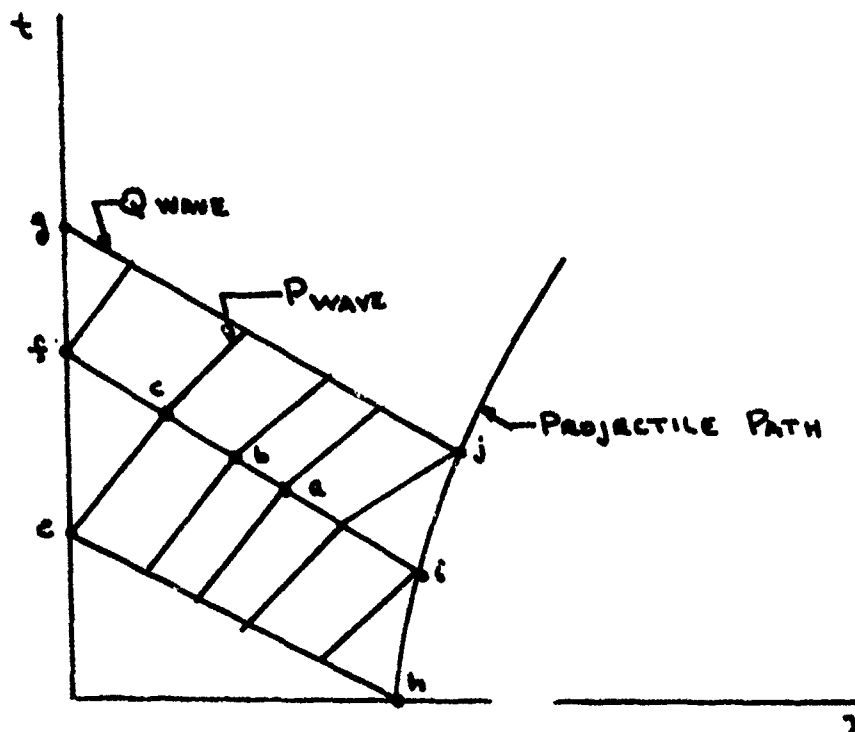


Figure 1: Schematic of Characteristic Grid Points

There are three types of grid points, interior points, (a,b,c), breach points (e,f,g) and projectile base points (h, i, j). The governing equations and solution procedures are different for each of these types of grid points and therefore, each will be handled separately.

Interior Points

Figure 2 shows a typical interior unknown grid point (6). It is on a P wave from point (4) and a Q wave from point (3).

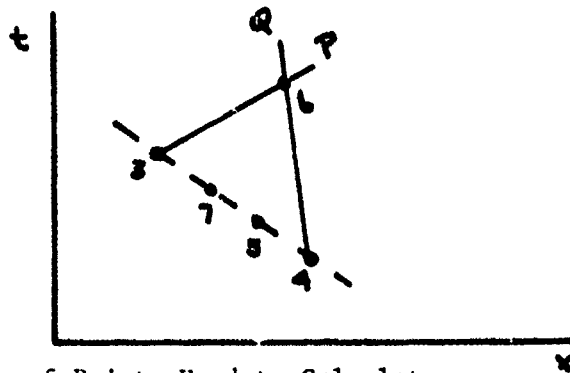


Figure 2: Diagram of Points Used to Calculate Interim Grid Points

Point (7) represents the location of a gas particle which intersects point (6) and the line connecting points (3) and (4). Point (5) is similar to point (7) except it represents a propellant particle. The slope of the P and Q characteristics are given by equations (12) and (13).

$$\frac{x_6 - x_3}{t_6 - t_3} = U_{g_{3,6}} + a_{3,6} \quad (12)$$

$$\frac{x_6 - x_4}{t_6 - t_4} = U_{g_{4,6}} - a_{4,6} \quad (13)$$

where

$$U_{g_{4,6}} = (U_{g_4} + U_{g_6})/2$$

$$a_{3,6} = (a_4 + a_6)/2$$

$$U_{g_{3,6}} = (U_{g_3} + U_{g_6})/2$$

$$a_{2,6} = (a_3 + a_6)/2$$

Solving for t_6 and x_6

$$t_6 = \frac{x_4 - x_3 + t_3(U_{g_{3,6}} + a_{3,6}) - t_4(U_{g_{4,6}} - a_{4,6})}{(U_{g_{3,6}} + a_{3,6}) - (U_{g_{4,6}} - a_{4,6})} \quad (14)$$

$$x_6 = x_3 + (U_{g_{3,6}} + a_{3,6})(t_6 - t_3) \quad (15)$$

Since the values at point 6 are initially unknown, an assumed value of a given parameter is used and then the procedure is repeated until the assumed value and calculated value agree to within a specified tolerance. The initial assumption is an arithmetic average of the values at points (3) and (4).

Knowing the location of point 6, it is possible using the procedure described in reference (8) in pages 23 through 30 to generate the data required for the solution to proceed. For brevity, the details will be omitted; however, certain key points should be mentioned. The average burning rate between points (5) and (6) given by:

$$r_{s,6} = B P_{s,6}^n (1 + k (U_g - U_{p,s,6} - 500))$$

The distance burned normal to a particle surface at (6) is:

$$x_6 = x_5 + r_{s,6} (t_6 - t_5)$$

Knowing x_6 and x_5 the average particle volume and surface area between (5) and (6) can be determined

$$V_{p5,6} = (V_{p5}(x_5) + V_{p6}(x_6))/2$$

$$S_{p5,6} = (S_{p5}(x_5) + S_{p6}(x_6))/2$$

The gas per unit length generated along the propellant path (5) and (6) is

$$\dot{m}_{g_{s,6}} = \left(\frac{\epsilon_{s,6}}{V_{p_{s,6}}} \right) S_{p_{s,6}} r_{s,6} \rho_p A$$

The rate of change in propellant particle velocity between (5) and (6) is given by equation (16)

$$\frac{DU_p}{Dt} = \frac{U_{p5,l} \dot{m}_{g5,l}}{\rho_p A E_{5,l}} + \frac{F_{d5,l}}{\rho_p E_{5,l}} \quad (16)$$

The rate of change of propellant particle volume fraction is given by equation (17)

$$\begin{aligned} \frac{De}{Dt} = & -\frac{e_{5,l}}{U_{p5,l}} \frac{DU_p}{Dt} - \frac{2 E_{5,l} U_{p5,l} (A_4 - A_5)}{(A_4 + A_5) (X_4 - X_5)} \\ & - \frac{\dot{m}_{g5,l}}{A \rho_p} \end{aligned} \quad (17)$$

The rate of entropy change for the gas can now be computed using equation (6). The change in P and Q along the appropriate characteristic is given by equations (18) and (19)

$$P_6 = P_5 + \frac{\delta_+ P_{5,l}}{\delta t} (t_6 - t_5) \quad (18)$$

$$Q_6 = Q_4 + \frac{\delta_- Q_{4,l}}{\delta t} (t_6 - t_4) \quad (19)$$

where $\delta_+ P_{5,l}/\delta t$ and $\delta_- Q_{4,l}/\delta t$ are given the equations (20) and (21)

$$\begin{aligned} \frac{\delta_+ P_{5,l}}{\delta t} = & -\frac{2 a_{5,l} U_{p5,l} (A_4 - A_5)}{(A_4 + A_5) (X_4 - X_5)} + \frac{(\beta - 1) a_{5,l} g J}{\gamma R} \frac{Ds}{Dt} \\ & + \frac{a_{5,l} g J}{\gamma R} \left[\frac{Ds}{Dt} + a_{5,l} \frac{(s_6 - s_5)}{(X_6 - X_5)} \right] - \frac{\tau_w \pi D}{A (1 - e_{5,l}) \rho_{g5,l}} \\ & + \frac{a_{5,l}}{(1 - e_{5,l})} \left(\frac{De}{Dt} + \frac{a_{5,l}^2 \dot{m}_g}{A \rho_{p5,l} \gamma} \right) - \frac{i}{\rho_{g5,l} (1 - e_{5,l})} \left(F_d + \frac{U_{p5,l} \dot{m}_g}{A \rho_{p5,l}} \right) \end{aligned} \quad (20)$$

$$\begin{aligned}
\frac{\delta Q_{4,6}}{\delta t} = & - \frac{2 Q_{4,6} U_{g4,6}}{(A_4 + A_5)} \frac{(A_4 - A_5)}{(x_4 - x_5)} + \frac{(\gamma - 1)}{\gamma} \frac{Q_{4,6} g J}{R} \frac{DS}{Dt} \\
& + \frac{Q_{4,6} g J}{TR} \left[\frac{DS}{Dt} - Q_{4,6} \frac{(S_6 - S_4)}{(x_6 - x_4)} \right] + \frac{T_{4,6} TD}{A(1 - \epsilon_{4,6}) \rho_{g4,6}} \\
& + \frac{Q_{4,6}}{(1 - \epsilon_{4,6})} \left[\frac{DE}{Dt} + \frac{Q_{4,6}^2 \sin \theta}{A \rho_{4,6} \delta} \right] + \frac{1}{\rho_{g4,6} (1 - \epsilon_{4,6})} \left[F_d + \frac{U_{g4,6} \sin \theta}{A \rho_{g4,6}} \right] \quad (21)
\end{aligned}$$

Using the calculated values for P_6 and Q_6 , new values for the gas velocity and speed of sound can be computed

$$U_{g6} = (P_6 - Q_6) / 2 \quad (22)$$

$$a_6 = \left(\frac{\gamma - 1}{4} \right) (P_6 + Q_6) \quad (23)$$

The entropy at point 6 can be calculated from equation (24)

$$S_6 = S_7 + \left(\frac{DS}{DT} \right) (t_6 - t_7) \quad (24)$$

The new values of U_{g6} , a_6 , and S_6 can be used to calculate the remaining thermodynamic properties based upon the equations on page 34 reference 8.

In addition U_{g6} and a_6 are available to obtain a new estimation of the location of point (6) (i.e., t_6 , X_6). The procedure described above is then repeated until the new values of a_6 and U_{g6} agrees with the previously calculated ones to within a specified tolerance.

Projectile Base Point

The solution at the projectile base is determined by the intersection of a P wave and the path of the projectile. Figure 3 presents a diagram of this intersection. The location and thermodynamic properties at

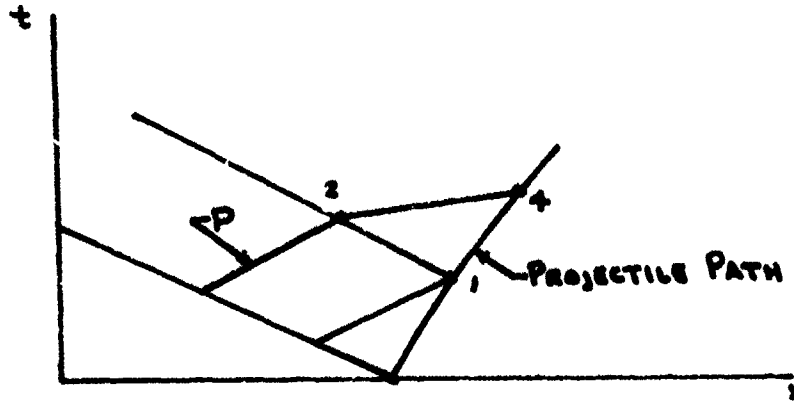


Figure 3: Diagram of Points Used to Calculate a Projectile Base Point

points 1 and 2 are known. This section describes the procedure to find point 4. The slope of the P wave from 2 to 4 is given by equation (25)

$$\frac{x_4 - x_2}{t_4 - t_2} = U_{g_{4,2}} + a_{4,2} \tag{25}$$

In addition integration of the equation of motion of the projectile yields equation (26)

$$x_4 = x_1 + U_{g_1}(t_4 - t_1) + \frac{1}{2} \left[\frac{(P_1 + P_4)}{2} \frac{g A}{W_t} - \frac{R_1 g}{W_t} \right] (t_4 - t_1)^2 \tag{26}$$

Simultaneous solution of equations (25) and (26) yields equation (27)

$$t_4 = \frac{-B - \sqrt{B^2 - 4AC}}{2A} \quad (27)$$

where

$$C = (x_1 - x_2) + (u_{g,3,4} + a_{z,4})t_2 - \left(\frac{(P_1 + P_2)gA}{2W_t} - \frac{R_1g}{W_t} \right) \frac{t_1^2}{2} \\ - t_1 (u_{g,1} - t_1 \left(\frac{gA(P_1 + P_2)}{2W_t} - \frac{R_1g}{W_t} \right))$$

$$B = u_{g,1} - \left(\frac{(P_1 + P_2)gA}{2W_t} - \frac{R_1g}{W_t} \right) t_1 - (u_{g,2,4} + a_{z,4})$$

$$A = \frac{1}{2} \left(\frac{(P_1 + P_2)gA}{2W_t} - \frac{R_1g}{W_t} \right)$$

Knowing t_4 , X_4 can be obtained from equation (25). At the base of the projectile the projectile velocity equals the gas velocity (eq. (28)).

$$u_{g,4} = u_{g,1} + \left(\frac{(P_1 + P_2)gA}{2W_t} - \frac{R_1g}{W_t} \right) (t_4 - t_1) \quad (28)$$

Having established a first approximation for the location and the velocity at point 4, the change in P along the characteristic 2-4 can be determined. The details regarding this procedure are given in reference 8, pages 36 to 40. The rates of change of P ($\partial P_{2,4} / \partial t$) and P4 are given by equations (29) and (30)

$$\begin{aligned}
 \frac{\delta_+ P_{3,4}}{\delta t} = & - \frac{2 a_{3,4} U_{g_{3,4}} (A_4 - A_2)}{(A_2 + A_4) (x_4 - x_2)} + a_{3,4} \frac{g J}{R} \frac{D S}{D t} \\
 & - \frac{\tau_w \pi D}{A (1 - \epsilon_{3,4}) \rho_{g_{3,4}}} + \frac{a_{3,4}}{(1 - \epsilon_{3,4})} \frac{D \epsilon}{D t} \\
 & - \frac{F_d}{\rho_{g_{3,4}} (1 - \epsilon_{3,4})} - \frac{U_{g_{3,4}} \dot{m}_{g_{3,4}}}{A (1 - \epsilon_{3,4}) \rho_{g_{3,4}}} \\
 & + \frac{a_{3,4}^3 \dot{m}_{g_{3,4}}}{A (1 - \epsilon_{3,4}) P_{3,4} \gamma}
 \end{aligned} \tag{29}$$

$$P_4 = P_2 + \frac{\delta_+ P_{3,4}}{\delta t} (t_4 - t_2) \tag{30}$$

Knowing P_4 and U_{g_4} , a new velocity of sound, a_4 , can be computed from equation (31)

$$a_4 = (P_4 - U_{g_4}) (\gamma - 1) / 2 \tag{31}$$

Using a_4 and s_4 , revised values for the other thermodynamic variable can be computed. The procedure is then repeated until the values of U_{g_4} and a_4 for two consecutive calculations agree within a specified tolerance.

After the projectile leaves the barrel the procedure is the same as described on pages 49 and 50 of reference 8. It is assumed that the gas velocity is sonic at muzzle exit and that Q waves after the projectile leaves, originate from the muzzle exit. Under these conditions X_{24} is fixed and the following relations exist:

$$t_4 = t_2 + \frac{(X_4 - X_2)}{(U_{g3,4} + a_{3,4})}$$

$$a_4 = \frac{P_4 (\gamma - 1)}{(\gamma + 1)}$$

$$U_{g4} = a_4$$

Breach Points

The breach is located at $X=0$. Figure 4 diagrams the intersection of a Q wave with the breach.

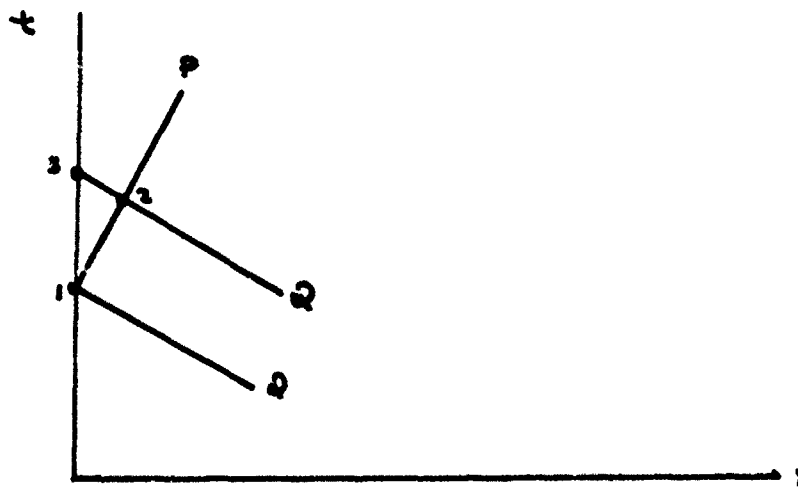


Figure 4: Diagram of Points Used to Calculate Breach Point

The time t_3 is given by equation (32)

$$t_3 = -X_2/U_{g2} - a_{2,3} + t_2 \quad (32)$$

In equation (32) the initial estimate of a_3 is made by assuming the same values as point (1). The change in Q from 2 to 3 is then computed and a revised a_3 can be obtained from equation (33)

$$a_3 = \frac{(\gamma-1)}{2} Q_3 \quad (33)$$

The rate of change of propellant volume fraction and of gas entropy are given by equations (34) and (35)

$$\frac{D\epsilon}{Dt} = -\frac{w_{ig}}{A\rho_p} - \epsilon \frac{\partial U_p}{\partial x} \quad (34)$$

$$\frac{DS}{Dt} = \frac{E_{gas} - R_{s1}}{A(1-\epsilon_{1,3})\rho_{g1,3}T_{g1,3}} \quad (35)$$

where

$$E_{g,23} = -g \pi D + g W \dot{m}_g$$

$$R_{23} = \dot{m}_g (g C_v T_{g,23}) + P_{1,3} \frac{A}{J} \frac{D\epsilon}{Dt} \\ + \frac{P_{1,3} \dot{m}_g}{\rho_{g,23} J}$$

The rate of change in Q along the characteristics from 2 to 3 is given by equation (36)

$$\frac{\delta Q_{2,3}}{\delta t} = a_{1,3} \frac{gJ}{R} \frac{D\delta}{Dt} + \frac{a_{1,3}}{(1-\epsilon_{1,3})} \frac{D\epsilon}{Dt} \\ + \frac{a_{1,3}^2 \dot{m}_g}{A(1-\epsilon_{1,3}) \rho_{g,23} J} \quad (36)$$

The value of Q and S at point 3 is given by equation (37) and (38)

$$Q_3 = Q_2 + \frac{\delta Q_{2,3}}{\delta t} (t_3 - t_2) \quad (37)$$

$$S_3 = S_1 + \frac{D\delta}{Dt} (t_3 - t_1) \quad (38)$$

Using equation (33) and (37), a new value of a_3 can be calculated. In addition, a_3 and S_3 can be used to calculate the remaining thermodynamic variables. The procedure is repeated until the value at a_3 from two successive calculations agrees within a specified tolerance.

The preceding procedure has been programmed and the details of the program are presented in Appendix A.

Flame Front Governing Equations

Initially it was assumed that there was instantaneous ignition of the entire propellant bed. This resulted in excessive breech pressure and low projectile base pressure. A better approximation is obtained by using a flame front with a finite velocity. Based upon the results from references (4) and (12), it was determined that the flame front velocity was proportional to the pressure behind the front. Using data from these references the following relationship was developed.

$$V_F = \alpha p^\beta \quad (39)$$

where

$$\begin{aligned} \alpha &= 31.5 \text{ in/sec/(spi)}^\beta \\ \beta &= .48 \end{aligned}$$

The effect of the flame front progressing through the propellant bed can then be determined by integrating from the breech to the projectile base. The pressure and temperature behind the flame front was assumed uniform. The gas velocity was also assumed to be zero. For a given time increment the distance the flame front moves is given by equation (40).

$$dL = \int_{t_1}^{t_2} V_F dt \quad (40)$$

In equation (40) the velocity is based upon the initial pressure (at t_1) and an assumed final pressure (at t_2). The procedure is repeated until the assumed final pressure and calculated final pressure agree to within 5%. The distance burned normal to the propellant surface in the same time period is given by equation (41)

$$d XL = (B p^n) (t_2 - t_1) \quad (41)$$

Using the results of reference (10) the new volume a propellant grain resulting from the surface recession given in equation (41) is

$$\begin{aligned} l_{i,j} &= l_{i,j-1} + dx_i \\ RL &= R_i - l_{i,j} \\ V_{i,j} &= 2\pi(RR^2)(RL) + \pi^2 RL^2 \left(RR + \frac{RL}{3} \right) \end{aligned} \quad (42)$$

where

$$RR = R_0 - R_i$$

R_0 = equivalent mean radius of propellant grain

R_i = one half web

The total gas generated in the cell defined by dL from the time $t = 0$ to $t = t_2$ is given by equation (43).

$$X_{mg} = dL \eta A (V_{oi} - V_{ij}) \rho_p \quad (43)$$

Equation (44) gives the volume fraction.

$$\epsilon_{ij} = (\eta AdL - X_{mg}/\rho_p) / (AdL) \quad (44)$$

The pressure behind the flame front is obtained by applying a modified perfect gas relationship to the total gas generated from every cell.

$$P = \frac{(XTC \cdot W + P_i A zL)}{(A zL - V_{ols} - XTC z)} \quad (45)$$

where

$\sum V_G$ = sum of gas generated in each cell at time t_2

Z_L = distance flame front has progressed from $t = 0$ to t_2

V_{ols} = total volume of solids behind flame front

V = propellant covolume

The pressure given by equation (45) applies to the entire region behind the flame front. This pressure is averaged with the pressure from the preceding time period to determine the flame front velocity. The procedure is repeated until the pressure in equation (45) for two successive passes agrees to within 5%

The flame front calculation procedure has been programmed and the details of the program as presented in Appendix B.

Heat Transfer Models

Since the analytical model considers the problem in three distinct regions, the breech, the interior, and the projectile base the heat transfer models will be considered in the same manner. The approach in defining the heat rates has been to use the best data either experimental or analytical.

Breech Region

In the breech region, the hot gases stagnate and as such, no boundary layer is formed. Although there may be recirculation flows in this region, analytical description would be extremely difficult. However, there is data available on heating in the projectile case region. Reference (12) developed experimental data on the heating rate at various locations in ammunition case region or a function of time. Figure 5 presents the results from reference 12. To obtain the heating at the breech, the data in figure 5 was extrapolated to $x = 0$ and then replotted in figure 6. The peak heating occurs at .25 milsec with a value of 3.7 Btu/ft²sec. After reaching this peak value the breech heating decreases exponentially with time. Rather than trying to match the peak heating, the approach taken was to satisfy the long term heating by fitting the following equation to the data in figure 6.

$$q = K_1 e^{K_2 t} (T_g - T_w)$$

Using 1 and 2 milsec as the matching times, the following values for K_1 and K_2 were obtained:

$$K_1 = 3.24 \text{ Btu/ft}^2\text{sec}$$

$$K_2 = -587.78 \text{ sec}^{-1}$$

The dotted line in figure 6 gives the profile of the fitted curve. To determine the effect of breech heating, the value of K_1 was varied from 0 to 3.24 on a series of computer runs. The results showed that breech heating had a negligible effect of projectile launch velocity and peak pressure.

HEAT TRANSFER DATA REF. 12

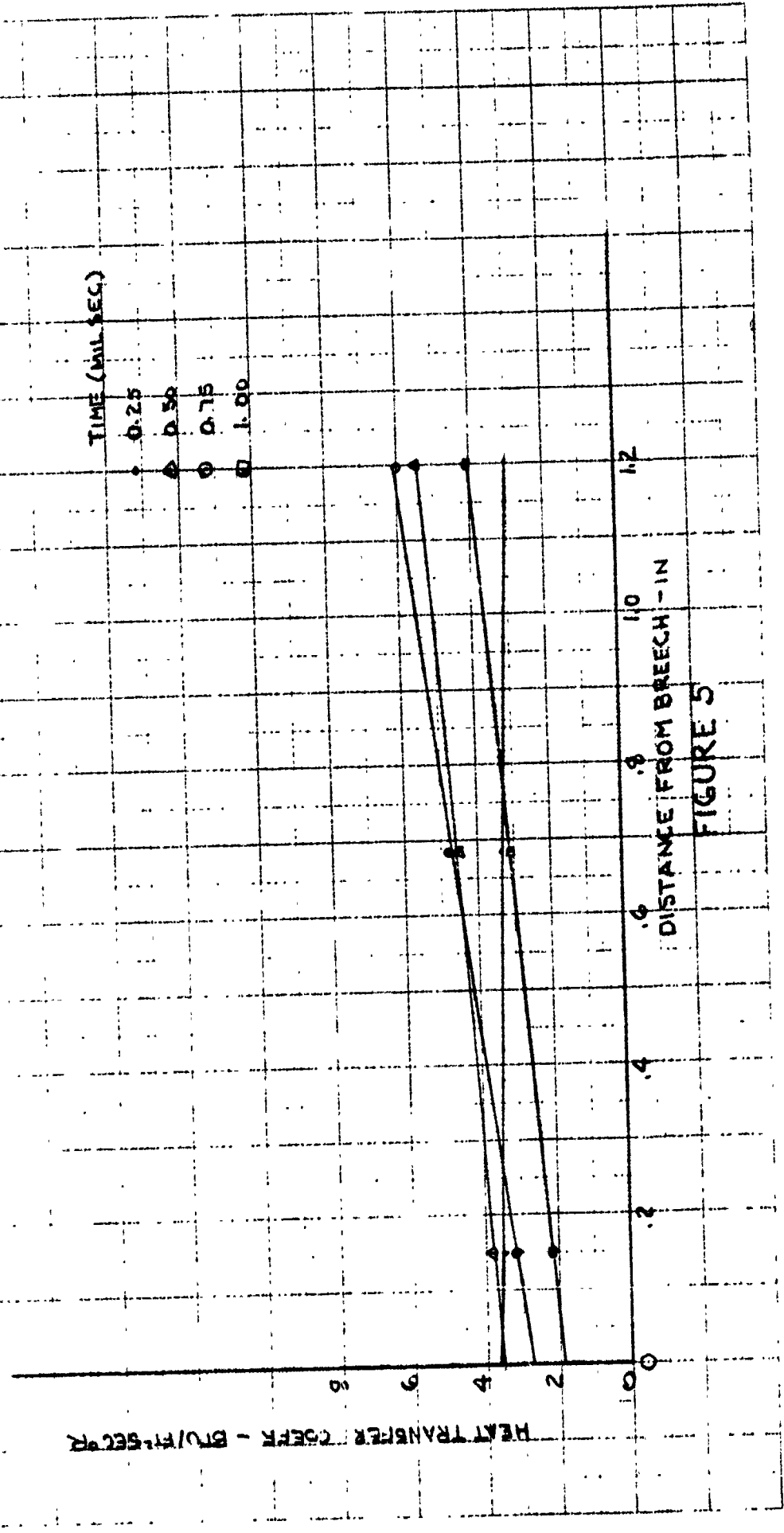


FIGURE 5

EXTRAPOLATION OF HEAT
TRANSFER DATA TO $x=0.0$

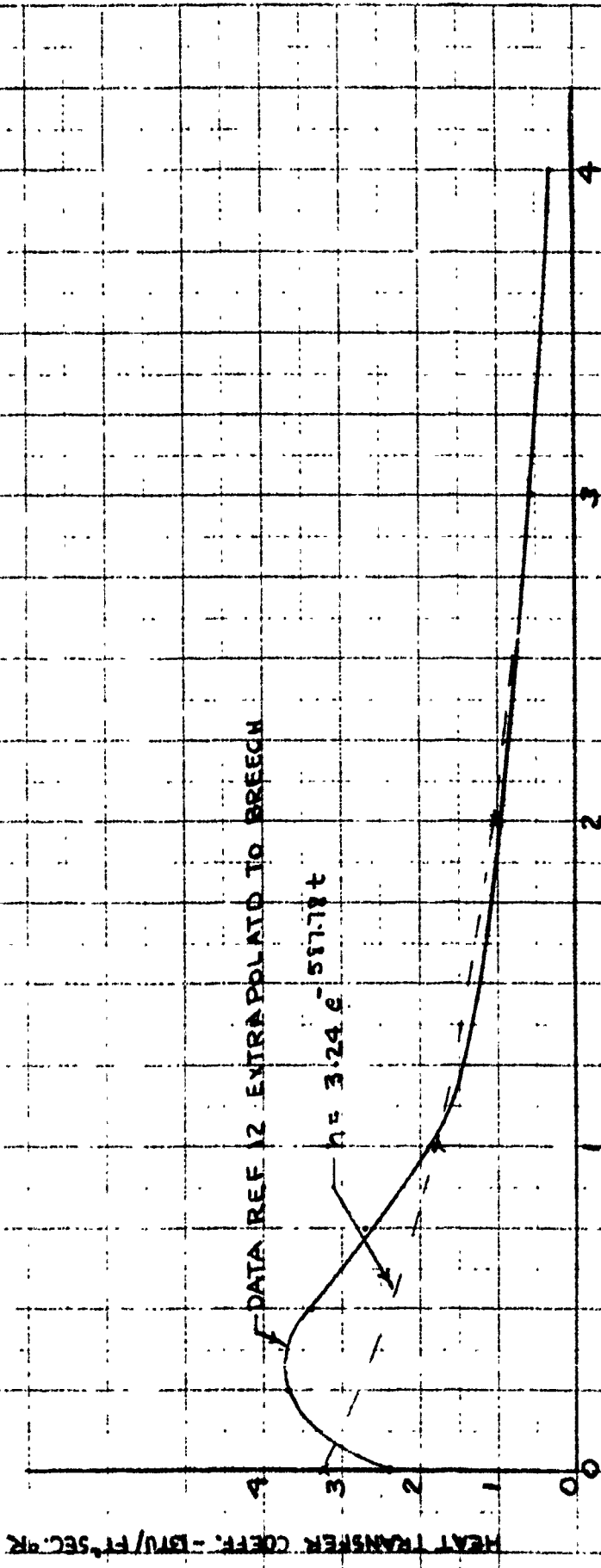


FIGURE 6

Interior Region

The interior region refers to those locations not considered to be the breech or projectile base. In the interior region, the boundary layer along the wall is fairly well defined. For this reason the approach has been to use the standard Reynolds Analogy:

$$\frac{h}{\rho V c_p} = \frac{f}{2}$$

The selection of the friction factor, f , is somewhat arbitrary but values between .001 and .006 have been used.

Projectile Base Region

Describing the heat transfer in this region is very difficult because the normal boundary layer approximations are not satisfied. In this region the gas velocity at the wall or base of the projectile equals the projectile velocity which is the highest velocity in the problem. In addition, the level of projectile heating (barrel heat transfer at projectile) has a profound effect upon the peak projectile base pressure and therefore, the launch velocity.

Initially, the approach was to simply use the Reynold Analogy in this region with the gas velocity equal to the projectile, velocity. However, this approach grossly underestimates the peak pressure at the base. Since the pressure increases with entropy decrease assuming constant gas temperature, this condition is valid as long as the propellant is burning. Entropy can be decreased by higher heat transfer rates. The approach taken therefore, was to arbitrarily increase the heat transfer coefficient. Factors of ten were necessary to significantly increase the base pressure. The requirement of a factor of this size seems unreasonable. In addition the peak heating rate occurs near the barrel exit which does not agree with test data.

The next approach was to use the heating rate based upon a shock tube end condition. This procedure was developed in reference (13). In this formulation the following equation was used:

$$h = \left(\rho_g \gamma C_p K \right)^{1/2} T_{gas} \left(.5 + .5 \left(\frac{T_w}{T_{gas}} \right)^2 - \frac{T_w}{T_{gas}} \right)^{1/2}$$

In this representation the shape of the heat transfer coefficient as a function of time is correct. However, the overall levels are too low. The constant, K, can vary by a factor of 2 (reference (13)) but this is still inadequate to predict the required levels of heating.

The most promising procedure is the one described in reference (3). In this reference the flow in the barrel is examined qualitatively and quantitatively. The reference notes that away from the projectile the Reynolds analogy could be used. However, in the projectile base region the momentum thickness goes to zero because the gas velocity and projectile velocity are equal. If a boundary layer analysis were attempted this would yield an infinite Nusselt number.

The approach taken in reference (3) was to use the usual boundary layer method away from the projectile and breech. These locations are handled using approximate solutions. The analysis develops the integral momentum equation and solves this equation introducing empirical data when needed. The projectile heat transfer is given by:

$$Nu = \frac{4 a^2 Re_c Pr^{1/2}}{Re_c}$$

where:

Nu = Nusselt Number hc_l/k

a = shear law constant = .332

Pr = Prandtl Number

Re_L = Reynolds Number based upon gas velocity and L

Re_{θ_t} = Reynolds Number based upon momentum thickness at transition

L = Distance from projectile to breech

The transition Reynolds Re_{θ_t} taken as 200. The heat transfer prediction method of reference (3) was used in the computer model because it provided the right profile and heat transfer rates of the right magnitude.

Numerical Results

Using the analysis described in the preceding sections, an analytical model computer program was developed and number of cases were examined. The most important parameter affecting the pressure and velocity history is the surface concentration density (SCD) of deterrent. Figures 7 and 8 present the pressure and velocity histories for an SCD of 0.1 and 0.2 respectively. In these two cases it is assumed that the flame velocity through the propellant bed is infinite. The surface concentration density of deterrent refers to the distribution of deterrent through the propellant grain. For all cases using the same propellant, the total amount of deterrent is the same; however, for an SCD of 0.1 compared to 0.2 the deterrent is spread to a greater grain depth. This means that the effect of the deterrent is less over a greater depth. For instance the SCD = 0.1 deterred flame temperature is 4615°R compared to 3331°R for an SCD = 0.2. From figure 7 it can be seen that the launch velocity for an SCD = 0.1 is 2500 fps. Launch occurs 1.27 milsec after ignition. For SCD = 0.2, (figure 8) the launch velocity is 1700 fps at 1.69 milsec. For both these runs the heat transfer rates at the projectile base were defined by the results of reference (3). Comparing the results from figure 7 and 8 with figure 1, the experimental data, it can be seen that considerable differences exist. In figure 7 the launch velocity and peak projectile base pressure are closer to the experimental results than figure 8. However, the launch velocity is only 78% of the measured data and the peak projectile pressure is only 59% of the corresponding experimental results. In contrast the peak breech pressure from figure 7 is 183% of the results in figure 1. It is felt that these differences can be attributed to:

- (1) projectile heat transfer
- (2) flame front velocity

Based upon earlier heat transfer studies it was determined that projectile heat transfer had a strong influence on projectile velocity and projectile base pressure. For comparison the projectile heat rate for an SCD of 0.1 and 0.2 are presented versus travel in figure 9. The peak projectile heating is $14,500 \text{ Btu/ft}^2 \text{ sec}$ at approximately 7 inches of travel. This is approximately one half the predicted peak from reference (3). In addition, the peak occurs further downstream than anticipated by reference (3) and experimental experience.

The large variation in peak breech pressure was attributed to the high flame speed. To examine this effect, a finite flame program was written and run. The analytical basis for this program was described earlier. Table 1 presents some results from the finite flame velocity analysis.

TABLE 1

	SCD = 0.1	SCD = 0.2	SCD = 0.1 [*]
Max Pressure behine projectile-psia	414081	14,720	16,972
Flame Travel Time - sec	$.595 \times 10^{-3}$	$.756 \times 10^{-3}$	$.731 \times 10^{-3}$

^{*}SCD=0.1 but 1/2 burning rate to simulate ignition delay

Figure 10 presents the volume fraction, ϵ , distribution versus distance for the same cases on Table 1.

The pressure and velocity history using a finite flame velocity is given in figure 11 for SCD=0.2. The launch velocity is increased by 400 fps and the projectile base pressure is increased slightly. The breech pressure is reduced significantly because the finite flame velocity analysis sets the volume fraction at the breech equal to zero. Figure 12 presents the same results for an SCD=0.1. The launch velocity in figure 12 is 3800 fps. The peak projectile base pressure is 64,500 psia. This represents a substantial change over the results in figure 7. The flat response of the

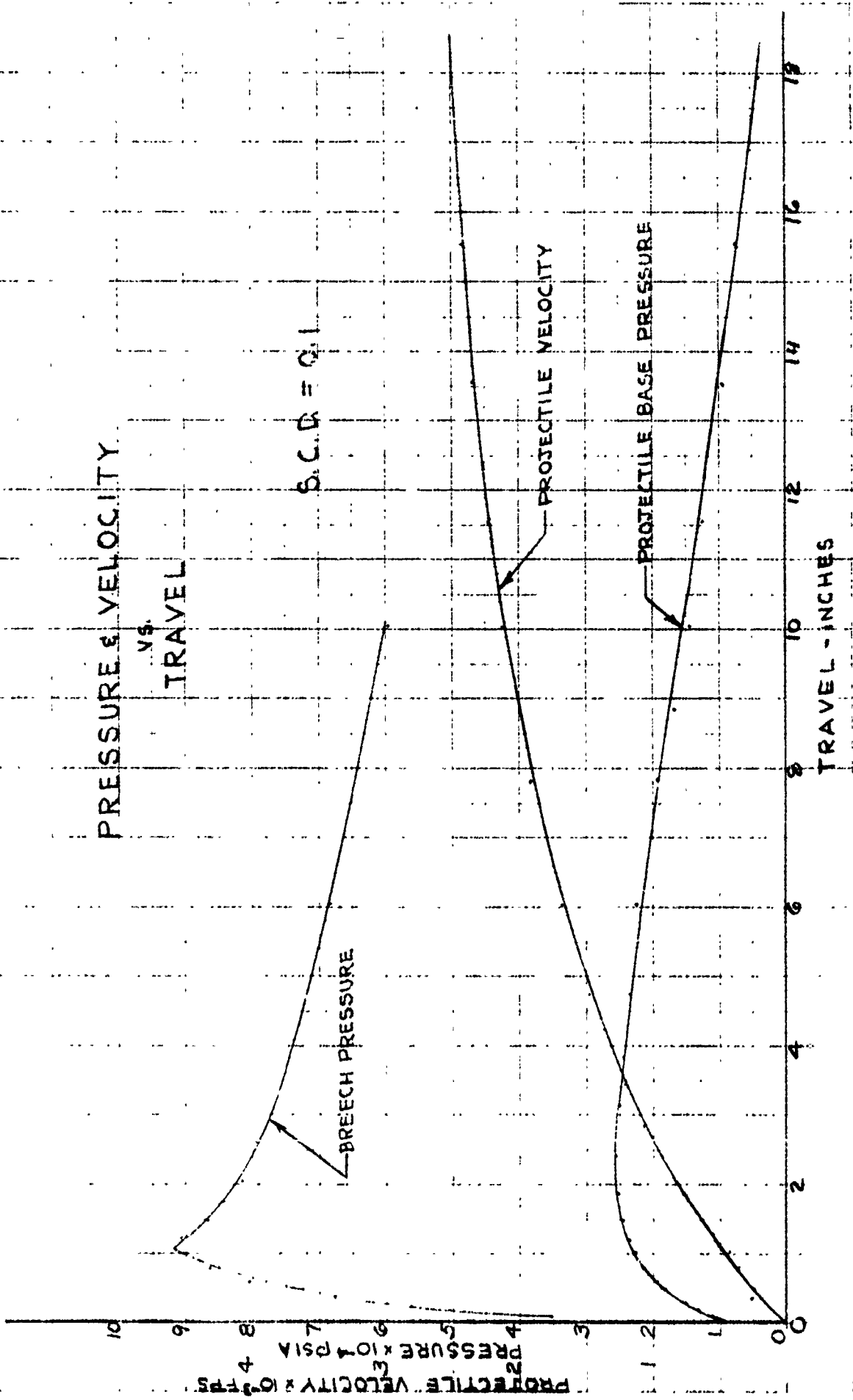
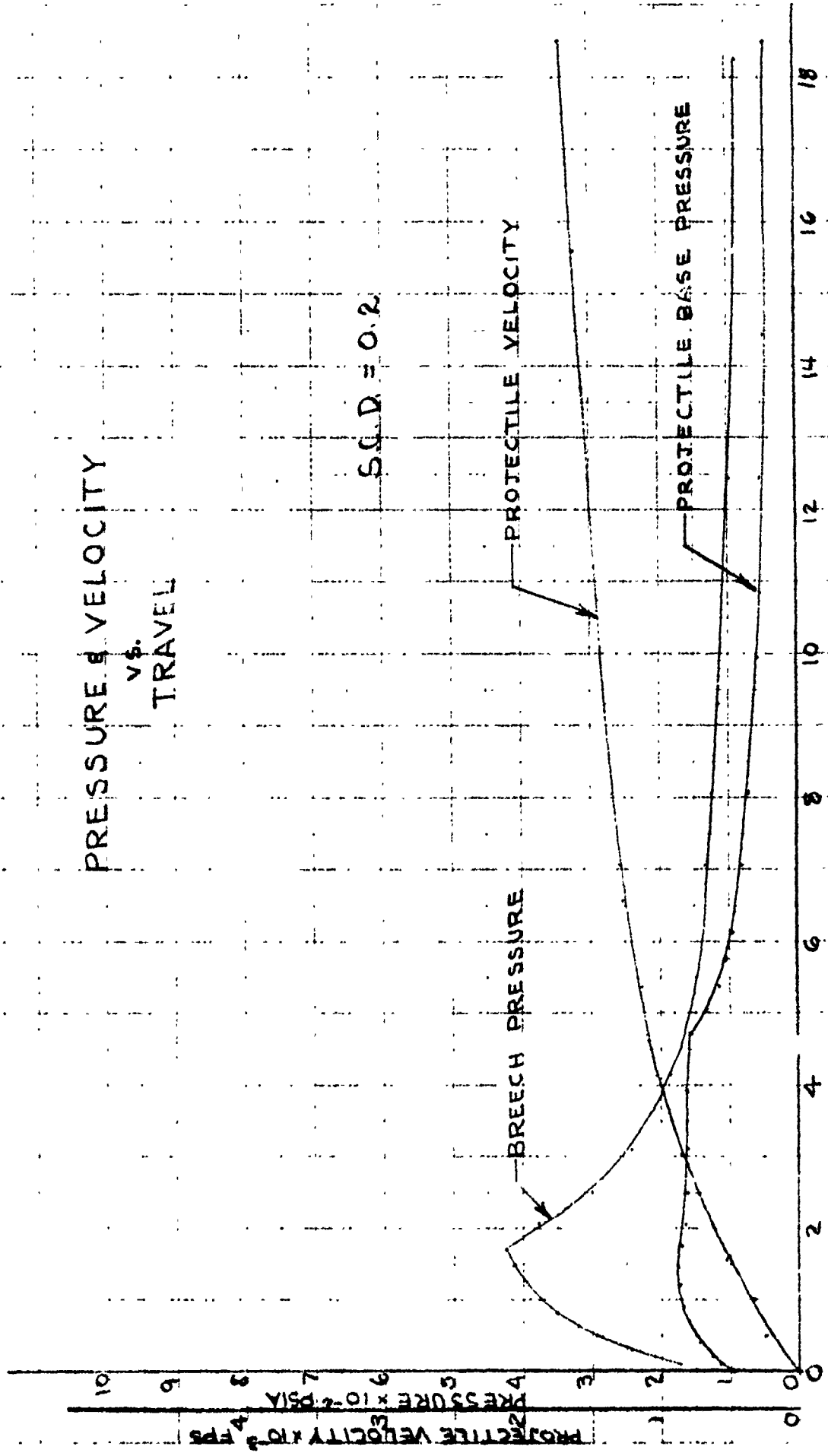


FIGURE 7



PRESSURE & VELOCITY
v.p.
TRAVEL

S.C.D. = 0.2

PROJECTILE VELOCITY

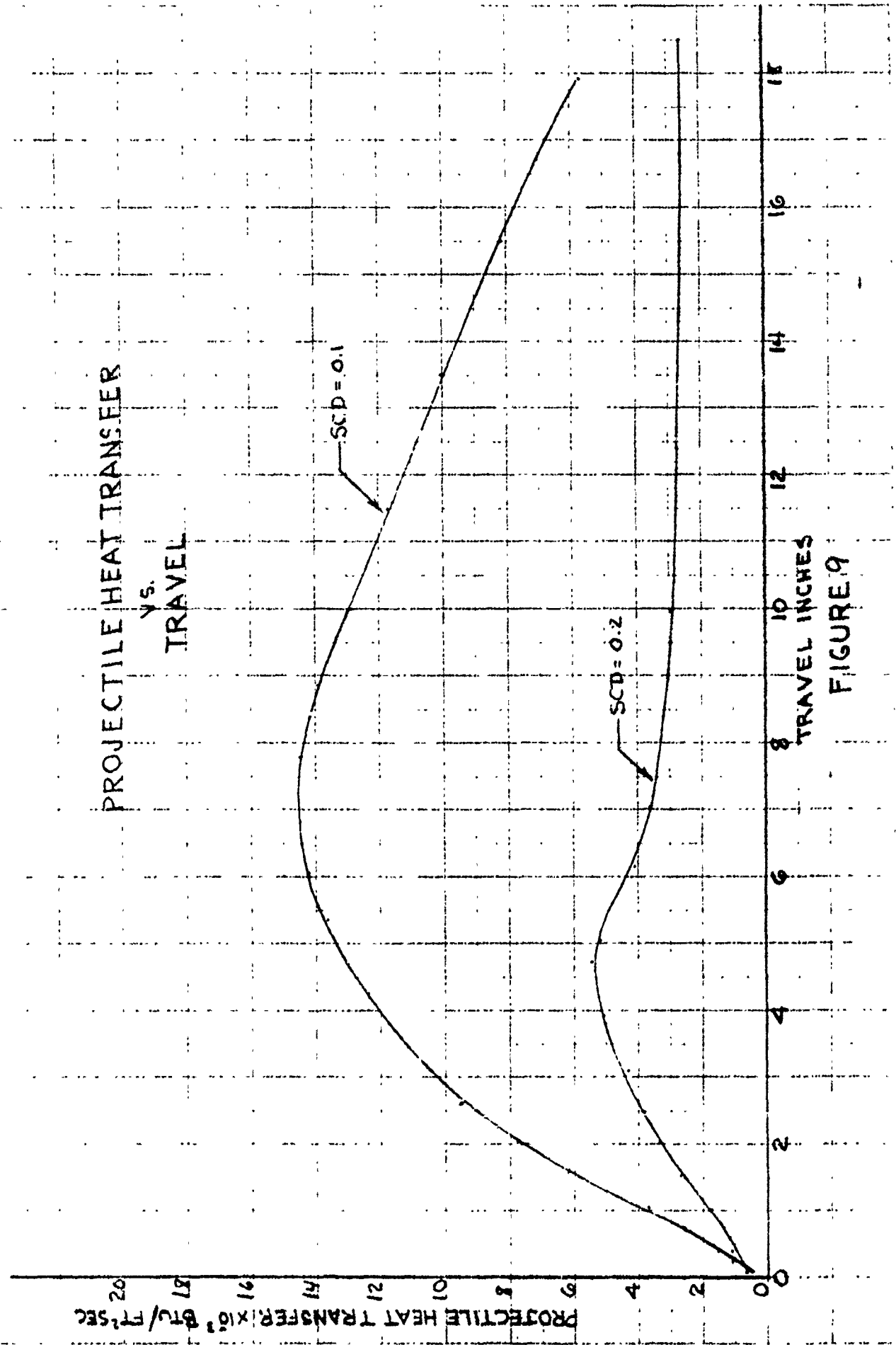
BREACH PRESSURE

PROJECTILE BASE PRESSURE

TRAVEL - INCHES

FIGURE 8

PROJECTILE HEAT TRANSFER
vs.
TRAVEL



TRAVEL INCHES
FIGURE 9

VOLUME FRACTION
vs.
DISTANCE FROM
BREACH

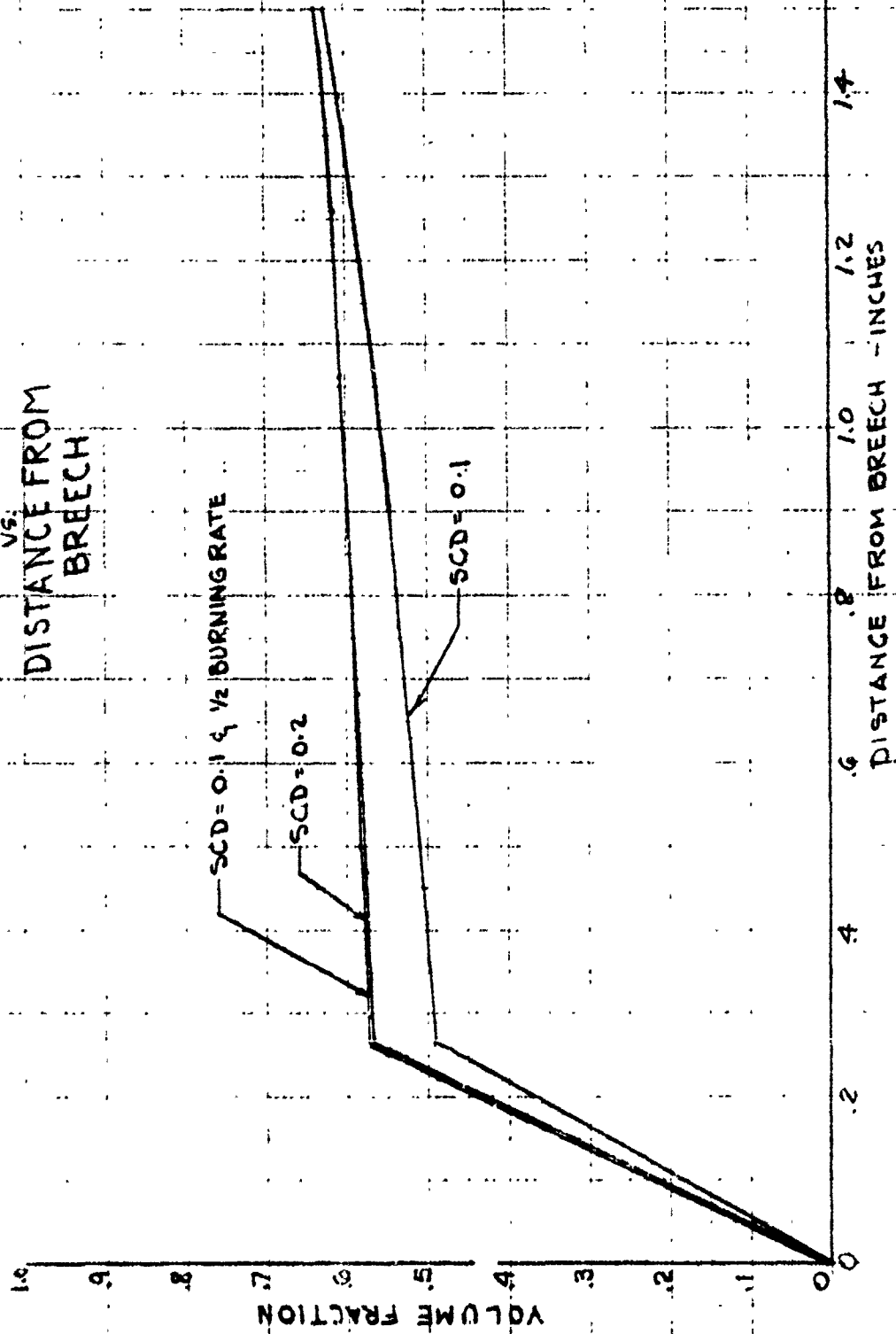


FIGURE 10

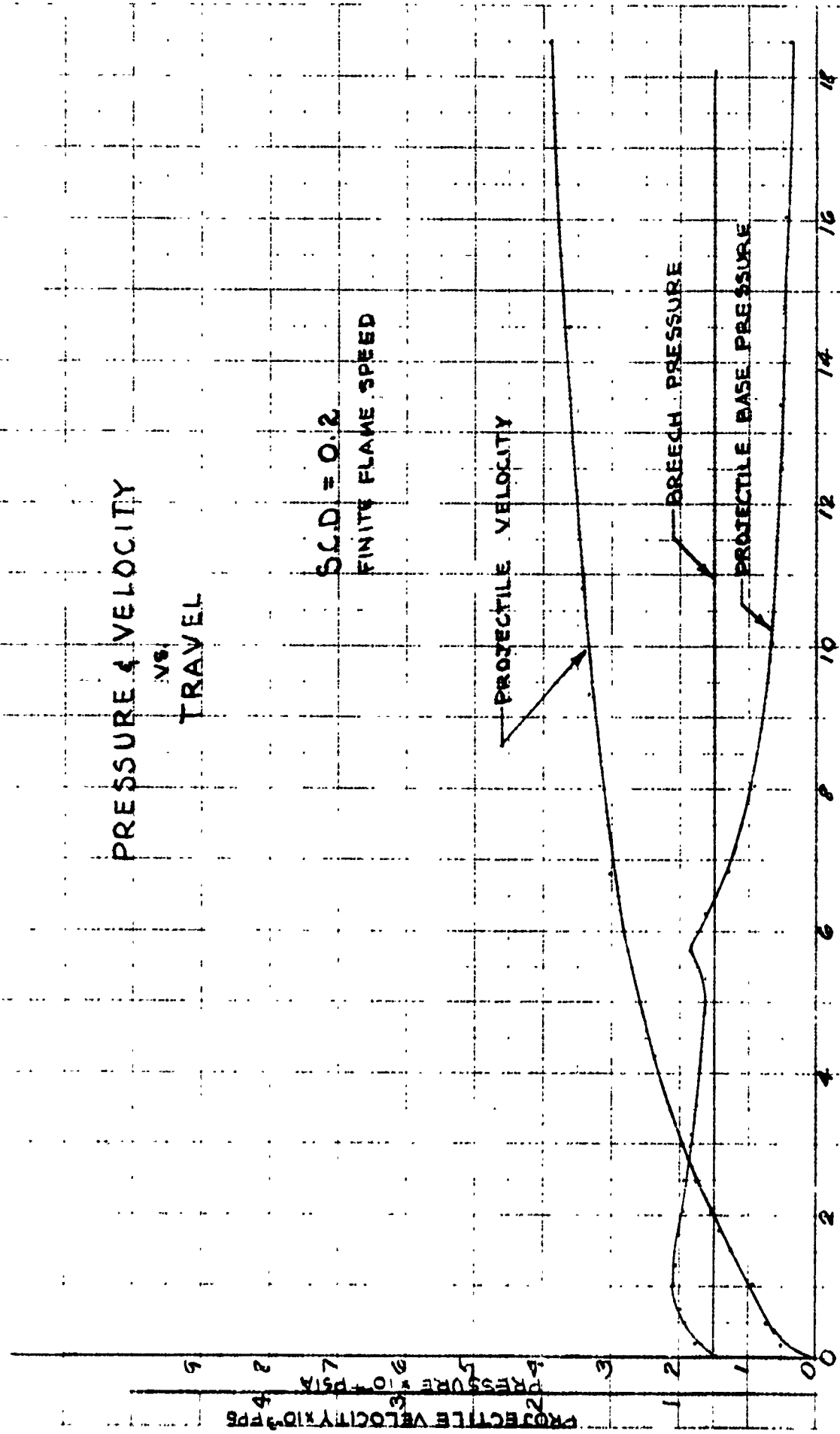


FIGURE III

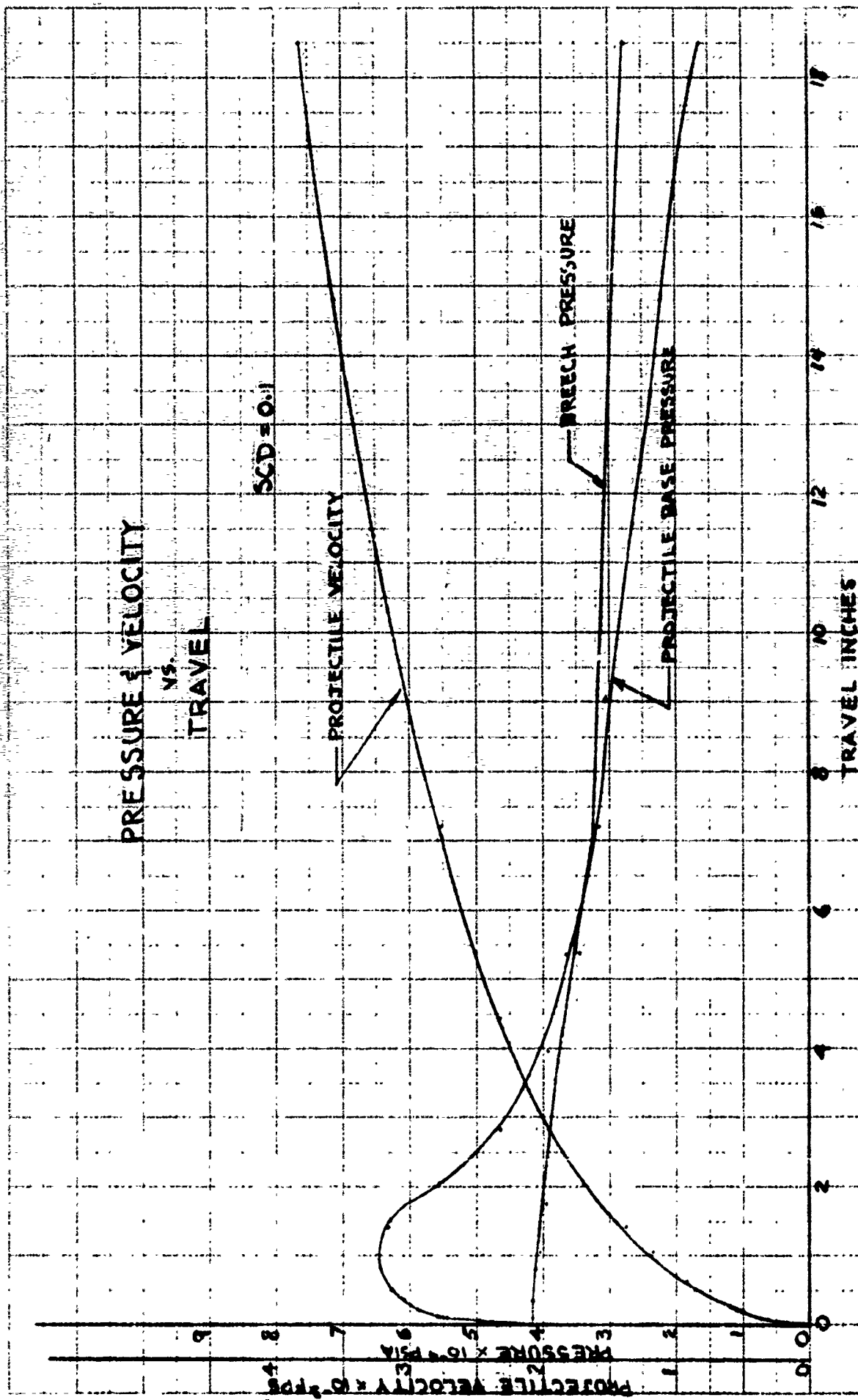
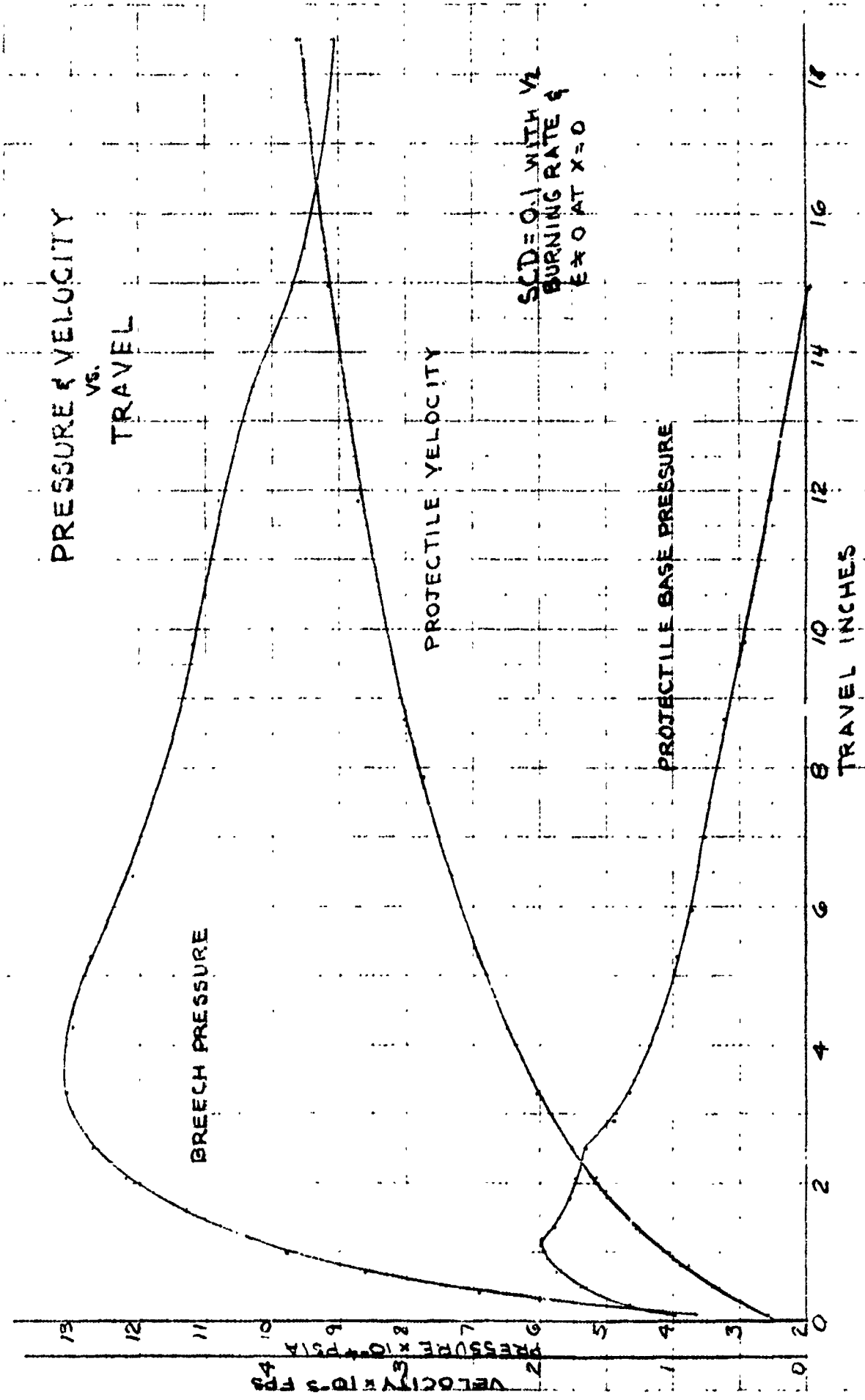


FIGURE 12

breech pressure curve is again attributed to the zero volume fraction at the breech.

To eliminate the flat response at the breech when using the finite flame criteria, it was decided to set the volume fraction at breech equal to the first station in the flame front analysis. This change increases the breech pressure significantly. For an SCD of 0.1, the results are not reasonable. To moderate this effect, the one half burning rate was used in the flame front analysis (see Table 1). With the breech volume fraction equal to zero, the peak breech pressure was approximately 17,000 psia. The peak projectile bore pressure and launch velocity were 57,500 psia and 3640 fps respectively. Figure 13 presents the complete pressure and velocity history for the non zero breech volume fraction. In this figure it can be seen that the peak breech pressure is 130,000 psia. This is approximately twice the experimental results. For this case the starting breech volume fraction was 0.574. A lower value would reduce this pressure.

Regarding the choice of heat transfer model, a number of runs were made using the usual Reynolds analogy. The results from these runs yielded launch velocities and pressure at the projectile well below test data. Some parametric runs were made to determine the necessary increase in heat transfer required to yield agreement with test. These results indicated a factor of 10 or 20 which does not seem reasonable. In addition the general shape of the profile predicted by the Reynolds analogy is incorrect. The Reynold's heating peaks with peak velocity. This means that peak heating would occur near launch. For this reason, the decision was made to use the heat transfer model described in reference (3) exclusively.



Conclusions and Recommendations

Computer models have been used to describe the flow field in small arms and also to describe the propagation of flame front through a porous propellant bed. The model determines the pressure, velocity, propellant volume fraction, and temperature versus time and position.

Numerical results have shown the dependence of projectile velocity and barrel pressure history upon deterrent concentration density and flame velocity. It has also been determined that the heat transfer to the base of the projectile also has a significant effect upon the launch condition.

Unfortunately, it was not possible to simulate the experimental data presented in figure 1. However, with some additional effort, the author feels that the results of figure 1 can be duplicated. Toward this goal, the following recommendations are made:

- (1) Vary breech volume fraction to simulate breech pressure.
- (2) Parametric study of projectile base heat transfer to obtain a steeper pressure profile.
- (3) Parametric study of projectile resistive force.
- (4) Development of analytical equations for flow at the base of the projectile.

References

- (1) Goldstein, S., "Study of the Pressure Distribution Behind the M193 Projectile When Fired in the M16 Rifle Barrel"
Report R-2066, Frankford Arsenal, Jan., 1973
- (2) Trafton, T. R., "An Improved Interior Ballistic Model for Small Arms Using Deterred Propellant", BRL Report 1624, USA Ballistic Research Lab, Nov., 1972.
- (3) Dahn, T. J., and Anderson, L. W., "Propellant Gas Convective Heat Transfer in Gun Barrels" Technical Report SWERR-TR-72-43, Weapons Laboratory at Rock Island, June, 1972 (AD747770)
- (4) Saha, Pradip, "An Analytical Study of the Interior Ballistics Problem, Including Movement of Solids and Wall Heat Transfer", Master Thesis Georgia Institute of Technology, Sept., 1971.
- (5) Kuo, K. K., Vechnevetsky, R., and Summerfield, M., "Generation of an Accelerated Flame Front in a Porous Propellant", AIAA Paper 71-210, Jan., 1971.
- (6) Kitchens Jr., Clarence W., "Flame Spreading in Small Arms Ball Propellant", BRL 1604, August, 1972. (AD750567)
- (7) Joglekar, A. M., Phadke, M. S., and Wu, S. M., "Iterative Modeling of Interior Ballistics of Small Arms", JI. of Spacecraft and Rockets, July, 1973.
- (8) Goldstein, S., "Behavior Model for the Propellant Gases in the Barrel of the M16A1 Rifle", Sept., 1971, (to be published).
- (9) Rudinger C., "Nonsteady Duct Flow: Wave Diagram Analysis", Dover.
- (10) Goldstein, S., "A Simplified Model for Predicting the Burning Rate and Thermochemical Properties of Deterred Rolled Ball Propellant", TN-1184, Frankford Arsenal

- (11) Goldstein, S., "Burning Rate Model for Nondeterred Rolled Ball Propellant", TN-1144, Frankford Arsenal, Feb., 1970.
- (12) Fisher E., "Determination of Temperature Gradients in 5.56 mm Aluminum Cases", Cornell Aeronautical Lab Report, Cal No GM-2962-Z-1 June, 1972.
- (13) Kemp, N., "Calculation of Heat Transfer from Similarity Boundary Layer Equations by a Simple Integral Method", AVCO Report BSD-TDR-62-171, June, 1962.

APPENDIX A
Description and listing of
Flow Model Computer Program

COMPUTER PROGRAM

The computer program implementing the numerical procedures described in preceding sections composed of a main program and 10 subprograms. The main program controls the flow of the calculation. The subprogram performs certain specific functions during the calculation. The name and function of each subprogram is given below:

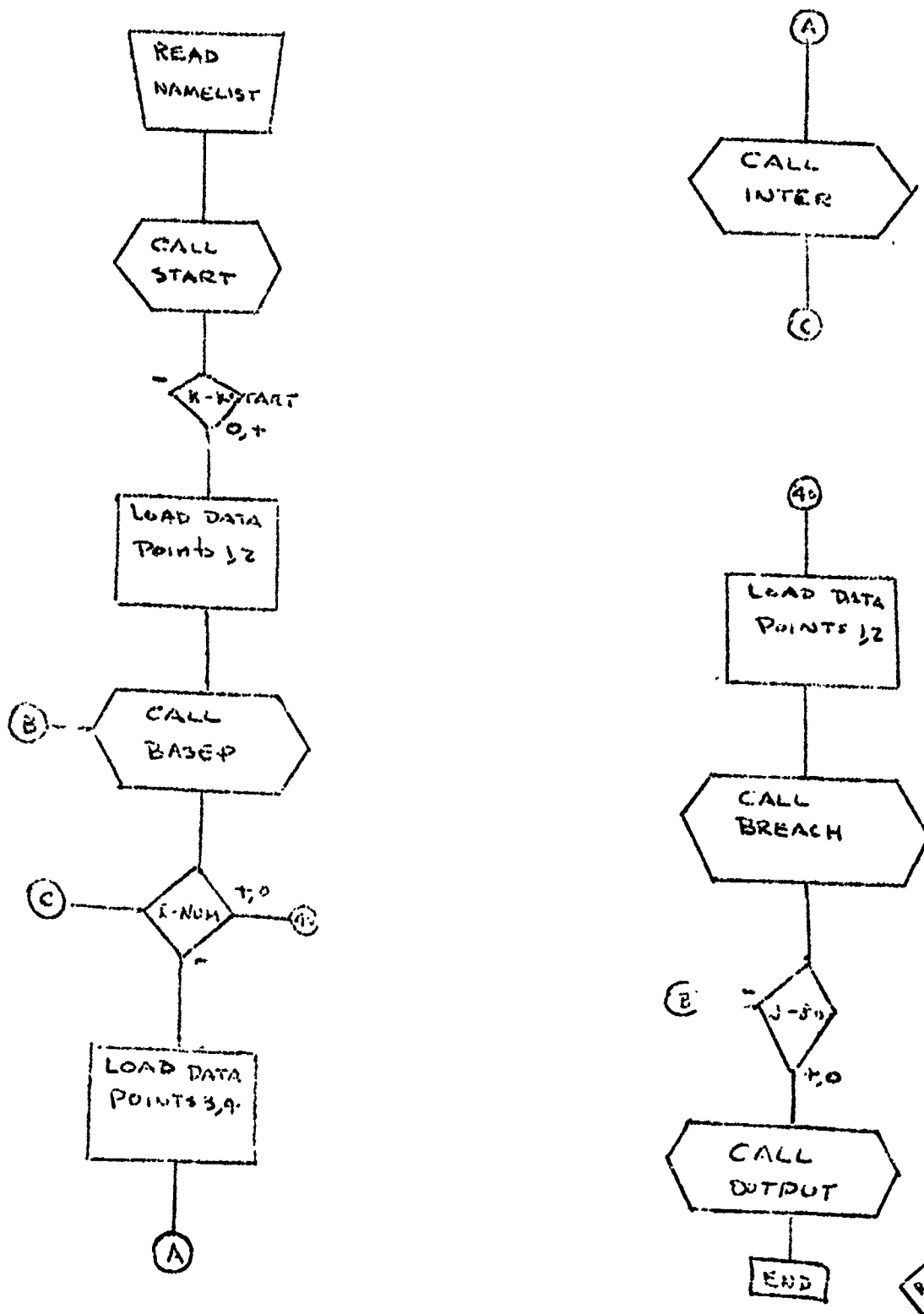
SUBPROGRAMFUNCTION

DIME	calculates the surface area, S_p , and volume, V_p , of propellant grain as a function of distance normal to the surface.
START	generates the pressure, entropy time history along the first Q wave from the starting point to the breach. The required number of points is specified in the input and program divides the distance from projectile base to breach into equal increments.
INTER	calculates the interior points using value at (3) and (4) (figure 2) as known
BREACH	calculates the breach points
BASEP	calculates the projectile base points
OUTPUT	points the required output information in the specified format
DIAGO	a diagnostic program which prints certain information if the calculations in INTER, BREACH, and BASEP do not converge within 10 tries
RFORCE	calculates the engraving force as to function of X based upon tabular input data
PROP	calculates the specific heat ratio, gas constant and specific heat at constant volume as a function of the amount of deterred and non-deterred propellant burned. The program is called only after the deterred layer is burned through

TAREA

This is a subjunction which calculates the tube cross sectional area as a function of X based on tabulated inputs.

The main program maintains control of the overall program and stores the calculated values of various parameters (i.e., gas velocity, propellant velocity, pressure, etc.) This data is stored in a double subscripted (i,j) array. When i equals j , the points correspond to the base of the projectile. Along a given Q wave the j subscript is constant. For a fixed value of j , the number of i values which determines the grid size is an input parameter. Figure 5 presents an abbreviated flow diagram for the main program.



Reproduced from best available copy.

FIGURE 5: FLOW DIAGRAM for Computer Program

DESCRIPTION OF ARRAYS AND VARIABLES

X(I,J)	X, location of grid points
TIME(I,J)	t, time of grid points
VEL(I,J)	gas velocity at grid points
SS(I,J)	speed of sound at grid points
PRESS(I,J)	pressure at grid points
TEMP(I,J)	gas temperature at grid points
DEWS(I,J)	gas density at grid points
VELP(I,J)	propellant velocity at grid points
ENTR(I,J)	entropy of gas at grid points
VOLFRA(I,J)	volume fraction at grid points
AL(I,J)	distance burned normal to propellant grain surface at grid points

The following are used in the main program and subroutine INTER (see Figure 2)

X3, X4, X6	spatial location of points 3, 4 and 6
T3, T4, T6	time location of points 3, 4 and 6
UG3, UG4, UG6	gas velocity at points 3, 4, and 6
A3, A4, A6	speed of sound at points 3, 4 and 6
PS13, PS14, PS16	gas pressure at points 3, 4 and 6
AREA3, AREA4, AREA6	tube cross sectional area at points 3, 4 and 6
TG3, TG4, TG6	gas temperature at points 3, 4 and 6
RHO3, RHO4, RHO6	gas density at points 3, 4 and 6

UP3, UP4, UP6	propellant velocity at points 3, 4 and 6
S3, S4, S6	entropy at points 3, 4 and 6
EPL3, EPL4, EPL6	propellant volume fraction at points 3, 4 and 6
L3, L4, L5, L6	distance burned normal to propellant grain at points 3, 4, 5 and 6

The following are used in the main program and subroutines BREACH and START (see figure 4)

X12	spatial location of point 2
T11, T12, T13	time location of point 1, 2 and 3
UG11, UG12, UG13	gas velocity at points 1, 2 and 3
A11, A12, A13	speed of sound at points 1, 2 and 3
PSI1, PSI2, PSI3	gas pressure at points 1, 2 and 3
TG11, TG12, TG13	gas temperature at points 1, 2 and 3
RHO11, RHO12, RHO13	gas density at points 1, 2 and 3
S11, S12, S13	entropy at points 1, 2 and 3
EPL11, EPL12, EPL13	propellant volume fraction at points 1, 2 and 3
AREA11, AREA12, AREA13	tube cross sectional area at points 1, 2 and 3
L11, L13	distance burned normal to propellant grain at points 1 and 3
UP12	propellant velocity at point 2

The following are used in the main program and subroutine BASEP (see Figure 3)

X21, X22, X24	spatial location of points 1, 2 and 4
T21, T22, T24	time location of points 1, 2 and 4

UG21, UG22, UG24	gas velocity at points 1, 2 and 4
A21, A22, A24	speed of sound at points 1, 2 and 4
PSI21, PSI22, PSI24	gas pressure at points 1, 2 and 4
TG21, TG22, TG24	gas temperature at points 1, 2 and 4
RHO21, RHO22, RHO24	gas density at points 1, 2 and 4
S21, S22, S24	entropy at points 1, 2 and 4
FPL21, EPL22, EPL24	propellant volume fraction at points 1, 2 and 4
AREA21, AREA22, AREA24	tube cross sectional area at points 1, 2 and 4
L21, L24	distance burned normal to the propellant surface at points 1 and 4
NSTART	the value of the I index for the Q wave

SUBROUTINES:

Name: INTER

Purpose: To calculate the characteristics and thermodynamic properties at any interior point in the mesh

Input: X3, X4, T3, T4, UG3, UG4, A3, A4, PSI3, PSI4, TG3, TG4, RH03, RH04, UP3, UP4, S3, S4, EPL3, EPL4, AREA3, AREA4, L3, L4

Output: X6, T6, UG6, A6, PSI6, TG6, TH06, UP6, S6, EPL6, AREA6,

Method: An iterative scheme is used until convergence to within a given tolerance is obtained. Normally, the convergence check is made on the calculated speed of sound and gas velocity. However, for gas velocities below 300 ft/sec only the speed of sound is checked. This procedure was necessary because below 300 ft/sec the accuracy requirements on P and Q for calculating gas velocity become excessive. At 300 ft/sec, a one percent error in the speed of sound can be translated into approximate a 10 percent in the gas velocity. At higher gas velocities, the percentage tolerance on gas velocity and speed of sound are the same.

Name: BREACH

Purpose: To calculate the characteristics and thermodynamic properties at the location X=0

Input: X12, T11, T12, UG11, UG12, A11, A12, PSI11, PSI12, TG11, TG12, RH011, RH012, S11, S12, EPL11, EPL12, AREA11, AREA12, L11, UP12

Output: T13, UG13, A13, PSI13, TG13, RHO13, S13, EPL13, L13

Method: An iterative scheme is used until convergence to within a given tolerance is obtained.

Name: BASEP

Purpose: To calculate the characteristics and thermodynamic properties at the base of the projectile and to locate the base of the projectile

Input: X21, X22, T21, T22, UG21, UG22, A21, A22, PSI21, PSI24,
TG22, RHO21, RHO22, S21, S22, EPL21, EPL22, AREA21, AREA22,
L21, NSTART

Output: X24, T24, UG24, PS124, TG24, RH024, S24, EPL24, AREA24, L24
 Method: An iterative scheme is used until convergence to within a given tolerance is obtained

Name: DIME (A, B, SURA, SURB, VOLA, VOLB)

Purpose: To calculate the average propellant grain surface area and volume

Input: A, B corresponding to the distance burned normal to the surface (R) at two points

Output: SURA, SURB surface of grain at respective points
 VOLA, VOLB volume of grain at respective points

Method: The following equations are used

$$\text{Volume} = 2\pi (\bar{R} - R_i)^2 (R_L - \lambda) + \pi^2 (R_L - \lambda)^2 \left((\bar{R} - R_i) + \frac{A}{3\pi} (R_L - \lambda) \right)$$

$$\text{Surface area} = 2\pi \left(\pi (R_L - \lambda) \left((\bar{R} - R_i) + \frac{2}{\pi} (R_L - \lambda) \right) + (\bar{R} - R_i)^2 \right)$$

name: OUTPUT

Purpose: To print the calculated results

Input: Calculated velocities and thermodynamic properties at all of the grid points

Output: Printed results including values of P and Q at each grid point

Method: Format of printed results specified in subroutine

Name: DIAGO (LA, BUG, AA)

Purpose: A diagnostic tool to print results calculated prior to Q failure to converge event

Input: LA indication of which subroutine failed LA=1 INTER
 LA=2 BASEP
 LA=3 BREACH

BUG last calculated gas velocity

AA last calculated speed of sound

Output: Printed output up to and including current value of thermo-
 dynamic variables

Method: Format used is specified in the subroutine

Name: RFORCE(A,B)

Purpose: Calculates the engraving force or a function of distance
 from initial projectile location

Input: A, location of the base of the projectile

Output: B, resistance force in lbf

Method: Resistance force tabulated or function of distance based upon
 data from Report R-2066, "Study of the Pressure Distribution
 Behind the M193 Projectile When Fired in the M16 Rifle Barrel"

Name: PROP(A)

Purpose: Calculates the CV, GAMMA, and RGAS as a function of the
 percentage deterred and non-deterred propellant burned.

Subroutine is used only when distance burned normal to the
 surface is greater than the deterred thickness of 0.00084 ft

Input: A distance burned normal to the propellant surface at a given
 mesh point

Output: CV, GAMMA, RGAS

Method: Calculation assumes the gas generated to be ideal and that
 properties are based upon mass fraction of components present

Reproduced from
 best available copy.

Name: START

Purpose: Calculates the thermodynamic properties along the first Q wave at specified intervals

Input: Same as BREACH but here they refer to data along first Q wave

Output: Same as BREACH but here they refer to data along first Q wave

Method: The subroutine is called a specified number of time (i.e. an input parameter). Each time it calculates the thermodynamic properties along the first Q wave. The results are equally spaced between the projectile initial location and the breach. The gas velocity and heat transfer along this wave are zero

SUBFUNCTION

Name: TAREA(ALOC)

Purpose: Calculates the tube cross sectional area as a function of distance from the breech

Input: ALOC location of the grid point

Output: TAREA tube cross sectional in ft^2

Method: Interpolates data from table which is supplied

C THIS PROGRAM CALCULATES THE PRESSURE,TEMPERATURE AND VELOCITY
C TIME HISTORIES BASED UPON A GIVEN PROPELLANT CHARACTERISTIC
C THIS IS THE MAIN PROGRAM

```

REAL L5,L6,L3,L4,L21,L24,L11,L13
COMMON/C/X(99,99),TIME(99,99),VEL(99,99),SS(99,99),PRESS(99,99),TE
SMP(99,99),DENS(99,99),VELP(99,99),ENTR(99,99),VOLFRA(99,99),AL(99,
999)
COMMON/COM1/X3,X4,X6,T3,T4,T6,UG3,UG4,UG6,A3,A4,A6,PSI3,PSI4,PSI6,
STG3,TG4,TG6,RHO3,RHO4,RHC6,UP3,UP4,UP6,S3,S4,S6,EPL3,EPL4,EPL6,ARE
>A3,AREA4,AREA6,L3,L4,L5,L6
COMMON/COM2/X12,T11,T12,T13,UG11,UG12,UG13,A11,A12,A13,PSI11,PSI12
S,PSI13,TG11,TG12,TG13,RHC11,RHO12,RHO13,S11,S12,S13,EPL11,EPL12,EP
*L13,AREA11,AREA12,AREA13,L11,L13,UP12
COMMON/COM3/X21,X22,X24,T21,T22,T24,UG21,UG22,UG24,A21,A22,A24,PSI
S21,PSI22,PSI24,TG21,TG22,TG24,RHC21,RHO22,RHO24,S21,S22,S24,EPL21,
)EPL22,EPL24,AREA21,AREA22,AREA24,L21,L24,NSTART
COMMON/SAME/RGAS,PSI1,GAMMA,DZERC,PIE,BEE,PODPOT,CV,BASE,GZERO,WT,
>TOL,AN
COMMON/STAR/KSTART
COMMON/OUT/MAXJ,MAXI
COMMON/EXIT/XLIM,TMUZE
COMMON/BHEAT/FACT,TWALL,FRICT
COMMON/PARM/PARIN1,PARIN2,PARIN3,PARBA1,PARBA2,PARBA3,PARBR1,PARBR
S2,PARBR3
COMMON/PCWDER/CV1,CV2,RGAS1,RGAS2,GAM1,GAM2,DLAY
NAMELIST/PAR/PARIN1,PARIA2,PARIN3,PARBA1,PARBA2,PARBA3,PARBR1,PARB
SR2,PARBR3
NAMELIST/INPOT/BASE,WT,TCL,XLIM,PSI1,DZERO,TZERO,XZERO,FRAC1,ALL1,
$FACT,TWALL,AN,FRICT,I,J
NAMELIST/PROPEL/PP1,PP2,CV1,CV2,BEE1,BEE2,RGAS1,RGAS2,DLAY,GAM1,GA
#P2

```

```

999 READ(5,INPOT)
READ(5,PAR)
READ(5,PROPEL)
WRITE(6,PROPEL)
WRITE(6,INPCT)
WRITE(6,PAR)
DO 1 II=1,99
DO 1 JJ=1,99
SS(II,JJ)=0.0

```

1

```

CONTINUE
TMUZE=1000.
PODPCT=PP1
CV=CV1
GAMMA=GAM1
BEE=BEE1
RGAS=RGAS1
PIE=3.141593
GZERC=32.2
TATM=530.
IF(I.GT.0)GC TO 20

```

C CALCULATION OF FIRST TWO POINTS

```

X(1,1)=XZERO
X(2,1)=0.0
TIME(1,1)=0.0
SS(1,1)=SQRT(GAMMA*RGAS*TZERO)
VOLFRA(1,1)=FRAC1
VEL(1,1)=0.0
VELP(1,1)=0.0
PRESS(1,1)=PSI1
TEMP(1,1)=TZERO
DENS(1,1)=PSI1/RGAS/TZERO
ENTR(1,1)=(RGAS/778.+CV)*ALOG(TZERO/TATM)-RGAS/778.*ALOG(PSI1/2075

```

```

#.)
ENTR(1,1)=ENTR(1,1)*778./RGAS/GAMMA
AL(1,1)=ALL1
IF(ALL1.GT.CLAY) BEE=BEE1
IF(ALL1.GT.CLAY) PODPOT=FP2
IF(ALL1.GT.CLAY)CALL PROP(ALL1)
KSTART=J
DO 3 I=1,KSTART
K=I+1
X12=X(I,1)
T12=TIME(I,1)
EPL12=VOLFRA(I,1)
A12=SS(I,1)
UG12=VEL(I,1)
UP12=VELP(I,1)
PSI12=PRESS(I,1)
TG12=TEMP(I,1)
RHO12=DENS(I,1)
S12=ENTR(I,1)
L11=AL(I,1)
CALL START
PRPSI=PSI13/144.
WRITE(6,5002)A13,L13,PRPSI,TG13,RHO13,S13,EPL13,T13
X(K,1)=X12
TIME(K,1)=T13
VOLFRA(K,1)=EPL13
SS(K,1)=A13
VEL(K,1)=UG13
VELP(K,1)=UG13
PRESS(K,1)=PSI13
TEMP(K,1)=TG13
DENS(K,1)=RHO13
ENTR(K,1)=S13
AL(K,1)=L13
3 CONTINUE
NCHECK=0
JLAST=1
5 DO 50 I=2,80
IF(NCHECK.GT.0)JLAST=JLAST+1
NCHECK=0
JQ=JLAST+1
DO 49 JJ=JQ,I
J=JJ
IF(JJ.EQ.I) GO TO 55
X4=X(I-1,J)
X3=X(I,J-1)
T4=TIME(I-1,J)
T3=TIME(I,J-1)
UG4=VEL(I-1,J)
UG3=VEL(I,J-1)
A4=SS(I-1,J)
A3=SS(I,J-1)
PSI4=PRESS(I-1,J)
PSI3=PRESS(I,J-1)
TG4=TEMP(I-1,J)
TG3=TEMP(I,J-1)
RHO4=DENS(I-1,J)
RHO3=DENS(I,J-1)
UP4=VELP(I-1,J)
UP3=VELP(I,J-1)
S4=ENTR(I-1,J)
S3=ENTR(I,J-1)
EPL4=VOLFRA(I-1,J)

```

```

EPL3=VOLFRA(I,J-1)
L4=AL(I-1,J)
L3=AL(I,J-1)
TOOL=(L3+L4)/2.
IF(TCOL.GT.CLAY) GO TO 10
GO TO 14
10 BEE=BEE2
PODPOT=PP2
CALL PROP(TCOL)
14 AREA3=TAREA(X3)
AREA4=TAREA(X4)
WRITE(6,5003)X3,X4,T3,T4,UG3,UG4,A3,A4,PSI3,PSI4,TG3,TG4,RHO3,RHO4
$,UP3,UP4,EPL3,EPL4,L3,L4,AREA3,AREA4
CALL INTER
RGAS=RGAS1
BEE=BEE1
GAMMA=GAM1
CV=CV1
PODPCT=PP1
PRPSI=PSI6/144.
WRITE(6,5002)A6,L6,PRPSI,TG6,RHO6,S6,EPL6,T6,X6,UG6,UP6
5002 FORMAT(1X,11E11.3)
X(I,J)=X6
TIME(I,J)=T6
VEL(I,J)=UG6
PRESS(I,J)=PSI6
TEMP(I,J)=TG6
DENS(I,J)=RHO6
VELP(I,J)=UP6
ENTR(I,J)=S6
VOLFRA(I,J)=EPL6
SS(I,J)=A6
AL(I,J)=L6
IF(X3.LE.0.0) GO TO 40
IF(T6.GE.TMUZE) GO TO 48
GO TO 49
55 L=JJ-1
NSTART=I-1
K=I
X21=X(NSTART,L)
X22=X(K,L)
T21=TIME(NSTART,L)
T22=TIME(K,L)
UG21=VEL(NSTART,L)
UG22=VEL(K,L)
A21=SS(NSTART,L)
A22=SS(K,L)
PSI21=PRESS(NSTART,L)
PSI22=PRESS(K,L)
TG21=TEMP(NSTART,L)
TG22=TEMP(K,L)
RHO21=DENS(NSTART,L)
RHO22=DENS(K,L)
S21=ENTR(NSTART,L)
S22=ENTR(K,L)
EPL21=VOLFRA(NSTART,L)
EPL22=VOLFRA(K,L)
L21=AL(NSTART,L)
IF(L21.GT.DLAY) BEE=BEE2
IF(L21.GT.DLAY) PODPCT=PP2
IF(L21.GT.DLAY) CALL PROP(L21)
AREA21=TAREA(X21)
AREA22=TAREA(X22)

```

```

CALL BASEP
NSTART=I
PODPOT=PP1
CV=CV1
GAMMA=GAM1
BEE=BEE1
RGAS=RGAS1
PRPSI=PSI24/144.
5001 WRITE(6,5001)A24,L24,PRPSI,TG24,RHO24,S24,EPL24,T24,X24,UG24
FORMAT(1X,10E11.3)
X(NSTART,J)=X24
TIME(NSTART,J)=T24
VEL(NSTART,J)=UG24
VELP(NSTART,J)=UG24
SS(NSTART,J)=A24
PRESS(NSTART,J)=PSI24
TEMP(NSTART,J)=TG24
DENS(NSTART,J)=RHO24
ENTR(NSTART,J)=S24
VOLFRA(NSTART,J)=EPL24
AL(NSTART,J)=L24
GO TO 49
40 NCHECK=1
II=I
X12=X(II,J)
T11=T13
T12=TIME(II,J)
UG11=0.0
UG12=VEL(II,J)
X.1=0.0
A11=A13
A12=SS(II,J)
PSI11=PSI13
PSI12=PRESS(II,J)
TG11=TG13
TG12=TEMP(II,J)
RHO11=RHO13
RHO12=DENS(II,J)
S11=S13
S12=ENTR(II,J)
EPL11=EPL13
EPL12=VOLFRA(II,J)
UP12=VELP(II,J)
L11=L13
IF(L11.GT.DLAY) BEE=BEE2
IF(L11.GT.DLAY) PODPOT=PP2
IF(L11.GT.DLAY) CALL PROP(L11)
AREA11=TAREA(X11)
AREA12=TAREA(X12)
CALL BREACH
RGAS=RGAS1
BEE=BEE1
GAMMA=GAM1
CV=CV1
PODPCT=PP1
PRPSI=PSI13/144.
WRITE(6,5002)A13,L13,PRPSI,TG13,RHO13,S13,EPL13,T13,X13
L=I+1
K=J
AL(L,K)=L13
TIME(L,K)=T13
SS(L,K)=A13
PRESS(L,K)=PSI13

```

```

TEMP(L,K)=TG13
DENS(L,K)=RHO13
VEL(L,K)=0.0
VELP(L,K)=0.0
ENTR(L,K)=S13
X(L,K)=0.0
VOLFRA(L,K)=EPL13
MAXJ=JJ
IF(T13.GE.TMUZE) GO TO 48
49 CONTINUE
48 MAXI=I
IF(T13.GE.TMUZE) GO TO 56
50 CONTINUE
56 CALL OUTPUT
MAXI=MAXI+1
DO 51 I=MAXJ,MAXI
WRITE(7,5003)X(I,MAXJ),TIME(I,MAXJ),VOLFRA(I,MAXJ),SS(I,MAXJ),VEL(
$ I,MAXJ),VELP(I,MAXJ),PRESS(I,MAXJ),DENS(I,MAXJ),ENTR(I,MAXJ),AL(I,
#MAXJ),TEMP(I,MAXJ)
5003 FORMAT(3E20.5)
51 CONTINUE
GO TO 999
20 NSTART=1
KSTART=J
JLAST=1
NCHECK=0
KK=J+1
DO 52 I=1,KK
READ(5,5003)X(I,1),TIME(I,1),VOLFRA(I,1),SS(I,1),VEL(I,1),VELP(I,1
$),PRESS(I,1),DENS(I,1),ENTR(I,1),AL(I,1),TEMP(I,1)
WRITE(6,5003)X(I,1),TIME(I,1),VOLFRA(I,1),SS(I,1),VEL(I,1),VELP(I,
#1),PRESS(I,1),DENS(I,1),ENTR(I,1),AL(I,1),TEMP(I,1)
52 CONTINUE
T13=TIME(KK,1)
A13=SS(KK,1)
PSI13=PRESS(KK,1)
TG13=TEMP(KK,1)
RHO13=DENS(KK,1)
S13=ENTR(KK,1)
EPL13=VOLFRA(KK,1)
L13=AL(KK,1)
GO TO 5
END

```

```

SUBROUTINE BASEP
C SUBROUTINE BASEP
REAL L5,L6,L3,L4,L21,L24,L11,L13
C THIS SUBROUTINE CALCULATES PCINTS AT THE BASE OF THE PROJECTILE
COMMON/COM3/X21,X22,X24,T21,T22,T24,UG21,UG22,UG24,A21,A22,A24,PSI
$21,PSI22,PSI24,TG21,TG22,TG24,RHC21,RHO22,RHO24,S21,S22,S24,EPL21,
)EPL22,EPL24,AREA21,AREA22,AREA24,L21,L24,NSTART
COMMON/SAME/RGAS,PSI1,GAMMA,DZERC,PIE,BEE,PODPOT,CV,BASE,GZERO,WT,
>TOL,AN
COMMON/EXIT/XLIM,TMUZE
COMMON/DHEAT/FACT,TWALL,FRICT
COMMON/PARM/PARIN1,PARIN2,PARIN3,PARBA1,PARBA2,PARBA3,PARBR1,PARBR
$2,PARBR3
DATA RHC1,REC,DELTT/3.1085,0.9,0.000005/
A1=SQRT(GAMMA*RGAS*530.)
XTRAV=(X21-0.125)*12.
WRITE(6,5000)PODPOT,CV,BEE,L21,XTRAV
ITRY=1
NSTART=NSTART+1
5 PSI24=PSI21

```

```

EPL24=EPL21
A24=A21
P22=2.*A22/(GAMMA-1.)*LG22
RHO24=RHO21
UG24=UG21
TG24=TG21
ABASE=BASE*(PSI24+PSI21)
10 SLOPEP=(UG22+A22+UG24+A24)/2.
CALL RFORCE(X21,R1)
C=X21-X22+SLOPEP*T22
WORK=(ABASE/2.-R1)*GZERO*T21/WT
C=C-WORK*T21/2.-T21*(UG21-WORK)
B=UG21-WORK-SLOPEP
A=(ABASE/2.-R1)*GZERO/WT/2.
5000 FORMAT(1X,'*****',//,1X,5E20.5)
T24=(-B-SQRT(B*B-4.*A*C))/2./A
X24=X22+SLOPEP*(T24-T22)
IF(X24.GE.XLIM) GO TO 75
11 AREA24=TAREA(X24)
AREA=(AREA24+AREA21)/2.
UGMN=(UG21+UG24)/2.
PSIMN=(PSI24+PSI21)/2.
BR=BEE*((PSIMN/144.)*AN)/12.
DPDX=0.0
DL=BR*(T24-T21)
L24=L21+DL
IF(L24.GT.0.000625)L24=0.000625
CALL DIME(L21,L24,SURF21,SURF24,VOL21,VOL24)
IF(VOL21.LE.0.00)SURF21=0.00
IF(VOL24.LE.0.00)SURF24=0.00
DBAR=DZERO-L24-L21
IF(DBAR.LE.0.000652)DBAR=0.00
DBAR=DBAR**3
FOR24=-PIE*DBAR*DPDX/6.
EPLMN=(EPL21+EPL24)/2.
VOLMN=(VOL21+VOL24)/2.
SURFMN=(SURF21+SURF24)/2.
IF(VOLMN.LE.0.00) GO TO 12
ETAMN=EPLMN/VOLMN
GO TO 13
12 ETAMN=0.00
13 CONTINUE
AMGMN=ETAMN*SURFMN*BR*RHCP*AREA
DUPDX=(UG24-UG21)/(X24-X21)
DEPLDT=EPL21*(1.-EPL21)*(RHO24-RHO21)/RHO21-(EPL21+(1.-EPL21)*RHO2
#1/RHO)*AMGMN*(T24-T21)/RHO21/AREA
DEPLDT=DEPLDT/(T24-T21)
14 CONTINUE
FD24=EPLMN*FOR24/VOLMN
RHOMN=(RHO24+RHO21)/2.
TGMN=(TG24+TG21)/2.
DIA=SQRT(4.*AREA/PIE)
AMN=(A22+A24)/2.
TAW=TGMN*(1.+REC*(GAMMA-1.)*UGMN*UGMN/2./AMN/AMN)
QHEAT1=0.00298*(CV**0.333)*RHOMN*UGMN
QHEAT=QHEAT1*(TGMN-TWALL)
EGAS=-QHEAT*PIE*DIA+AMGMN*PODPOT*GZERO
TAUW=0.0005*RHOMN*UGMN*UGMN
F1=UGMN*AMGMN*TAUW*PIE*CIA+FD24*AREA
F1=F1/778.
RS1=AMGMN*(CV*TGMN+UGMN*UGMN/1556.)+(AREA*DEPLDT
$+AMGMN/RHOMN)*PSIMN/778.
DSDT=AMGMN*(PODPOT*GZERO-(CV+RGAS/778.)*TGMN)+(TAUW*UGMN/778.-

```

```

#QHEAT)*PIE*DIA+FD24*UGMN*AREA/778.-PSIMN*AREA*DEPLDT/778.
DSDT=DSDT/AREA/RHOMN/TGMN/(1.-EPLMN)
AREA=(AREA24+AREA22)/2.
DELPDT=-AMN*UGMN*(AREA24-AREA22)/(X24-X22)/AREA
DELPDT=DELPDT+778.*AMN*DSDT/RGAS
WORK=(TAUW*PIE*DIA/AREA-AMN*RHOMN*DEPLDT+FD24+UGMN*AMGMN/AREA)/RHO
+MN/(1.-EPLMN)
WORK=WORK-(AMN*3)*AMGMN/AREA/(1.-EPLMN)/PSIMN/GAMMA
DELPDT=DELPDT-WORK
P24=P22+DELPDT*(T24-T22)
ANEW24=(P24-UG24)*(GAMMA-1.)/2.
TG24=(ANEW24*ANEW24)/GAMMA/RGAS
S24=S21+DSDT*(T24-T21)*778./RGAS/GAMMA
EPL24=EPL21+DEPLDT*(T24-T21)
IF(EPL24.LE.0.00)EPL24=0.0
WORK= 2.*GAMMA/(GAMMA-1.)
TG24=(ANEW24*ANEW24)/GAMMA/RGAS
PSI24=PSI21*((ANEW24/A21)**WORK)
PSI24=PSI24*EXP(-GAMMA*(S24-S21))
RHO24=PSI24/RGAS/TG24
ABASE=BASE*(PSI24+PSI21)
WORK=(ABASE/2.-R1)*GZERO/WT
UGNE24=UG21+WORK*(T24-T21)
CHECK=ABS((ANEW24-A24)/A24)
IF(CHECK.GT.TOL) GO TO 50
IF(UG24.LE.0.00) GO TO 50
CHECK=ABS((UGNE24-UG24)/UG24)
IF(CHECK.GT.TOL) GO TO 50
WRITE(6,5000)QHEAT2,QHEAT1,QHEAT,EGAS,RS1
XTRAV=(X24-0.125)*12.
DEL=AMGMN*PODPOT*GZERC-CV*TGMN)
WRITE(6,5000)L24,DEPLDT,CSCT,AMGMN,DEL,XTRAV
RETURN
50 ITRY=ITRY+1
IF(ITRY.LT.11) GO TO 200
LOC=2
CALL DIAGO(LOC,UGNE24,ANEW24)
200 UG24=UGNE24
A24=ANEW24
GO TO 10
75 X24=XLIM
300 FORMAT(1X,5E20.5)
T24=T22+(X24-X22)/SLOPEP
TMUZE=T24
GO TO 11
END
SUBROUTINE RFORCE(A,B)
DIMENSION XX(20),RF(20)
DATA XX/0.0,0.0333,0.0416,0.0499,0.066,0.100,0.1333,0.
>1666,0.200,0.2333,0.2666,0.300,0.333,0.500,0.6666,1.00,1.333,1.50,
$1.666,0.0/
DATA RF/0.0,520.,525.,520.,420.,255.,215.,195.,183.,17
>0.,162.,153.,145.,118.,95.,52.,18.,7.0,0.0,0.0/
A=A-0.1249
DO 10 I=1,19
IF(A.EQ.XX(I)) GO TO 15
IF(A.GT.XX(I).AND.A.LT.XX(I+1)) GC TO 20
10 CONTINUE
15 B=RF(I)
B=B/2.
A=A+0.1249
RETURN
20 SLOPE=(RF(I+1)-RF(I))/(XX(I+1)-XX(I))

```

```

C=RF(I)-SLOPE*XX(I)
B=<SLOPE*A+C
B=B/2.
A=A+0.1249
RETURN
END

```

SUBROUTINE BREACH

CSUBROUTINE BREACH

C THIS SUBROUTINE CALCULATES THE POINTS LOCATED ON THE BREACH

```

REAL L5,L6,L3,L4,L21,L24,L11,L13
COMMON/COM2/X12,T11,T12,T13,UG11,UG12,UG13,A11,A12,A13,PSI11,PSI12
$,PSI13,TG11,TG12,TG13,RHC11,RHO12,RHO13,S11,S12,S13,EPL11,EPL12,EP
*L13,AREA11,AREA12,AREA13,L11,L13,UP12
COMMON/SAME/RGAS,PSI1,GAMMA,DZERC,PIE,BEE,PODPOT, CV, BASE, GZERO, WT,
>TGL, AN

```

COMMON/EXIT/XLIP, TMUZE

COMMON/PARM/PARIN1, PARIN2, PARIN3, PARBA1, PARBA2, PARBA3, PARBR1, PARBR2, PARBR3

A1=SQRT(GAMMA*RGAS*530.)

ITRY=1

CONST=-0.58778E+03

TWALL=530.

UG13=0.0

A13=A11

RHOP=3.1085

AREA=AREA11

Q12=2.*A12/(GAMMA-1.)

PSI13=PSI11

EPL13=EPL11

30 SLOPEQ=(-A13+UG12-A12)/2.

T13=-X12/SLCPEQ+T12

IF(T13.GE.TMUZE) T13=TMUZE

PSIMN=(PSI13+PSI11)/2.

BR13=BEE*((PSIMN/144.)*AN)/12

DL13=BR13*(T13-T11)

L13=L11+DL13

IF(L13.GT.0.000625)L13=0.000625

CALL DIME(L11,L13,SURF11,SURF13,VCL11,VOL13)

IF(VOL11.LE.0.00)SURF11=0.00

IF(VOL13.LE.0.00)SURF13=0.00

EPLMN=(EPL13+EPL11)/2.

VOLMN=(VOL13+VOL11)/2.

IF(VOLMN.LE.0.00) GO TO 31

ETAMN=EPLMN/VOLMN

GO TO 32

31 ETAMN=0.00

32 CONTINUE

AMGMN=ETAMN*BR13*RHOP*AREA

AMGMN=AMGMN*(SURF13+SURF11)/2.

DEPLOT=-AMGMN/AREA/RHOP-EPLMN*UP12/X12

300 FORMAT(1X,5E20.5)

TG13=A13*A13/GAMMA/RGAS

TG#N=(TG13+TG11)/2.

RHC13=PSI13/RGAS/TG13

RHCMN=(RHO13+RHO11)/2.

DIA=SQRT(4.*AREA/PIE)

FILM=3.24*EXP(CONST*T13)*DIA/2./X12

QHEAT=FILM*(TG13-TWALL)

QHEAT=QHEAT*PARBR1

EGAS=-QHEAT*PIE*DIA+POCPCT*AMGMN*GZERO

RS1=AMGMN*(CV*TGMN+PSI#N/778./RHOP#N)+PSIMN*AREA*DEPLOT/778.

WORK=AREA*(1.-EPLMN)*R#OMN*TGMN

DSOT=AMGMN*(PODPOT*GZERO-(CV+RGAS/778.)*TGMN) -QHEAT*PIE*DIA -

```

#PSIMN*AREA*DEPLDT/778.
  DSDT=DSDT/WORK
  IF(T13.GT.PARBR2) GO TO 200
150 CONTINUE
  DELQDT=((A11+A13)/2.)*(778.*DSDT/REGAS+DEPLDT/(1.-EPLMN))
  DELQDT=DELQDT+((A11/2.+A13/2.)*3)*AMGMN/AREA/PSIMN/(1.-EPLMN)/GAM
  SMA
  Q13= Q12+DELQDT*(T13-T12)
  P13=Q13
  ANEW13=(GAMMA-1.)*Q13/2.
  TG13=ANEW13*ANEW13/GAMMA/REGAS
  S13=DSDT*(T13-T11)*778./REGAS/GAMMA+S11
  PSI13=PSI11*((ANEW13/A11)**(2.*GAMMA/(GAMMA-1.)))
  PSI13=PSI13*EXP(-GAMMA*(S13-S11))
  RHC13=PSI13/REGAS/TG13
  EPL13=EPL11+DEPLDT*(T13-T11)
  IF(EPL13.LE.0.00)EPL13=0.0
  CHECK=ABS((ANEW13-A13)/A13)
  A13=ANEW13
  IF(T13.GE.TMUZE)RETURN
  IF(CHECK.GT.TOL) GO TO 180
  RETURN
180 ITRY=ITRY+1
  IF(ITRY.LT.11) GO TO 30
  LOC=3
  CALL DIAGO(LJC,UG13,A13)
  RETURN
200 WRITE(6,300)L11,L13,VOL11,VOL13,SURF11,SURF13,EPLMN,ETAMN,AMGMN,DE
  #PLDT,QHEAT,EGAS,DSDT,AREA
  GO TO 150
  END
  SUBROUTINE DIAGO(LA,BUG,AA)
C THIS IS A DIAGNOSTIC SUBROUTINE
  REAL L5,L6,L3,L4,L21,L24,L11,L13
  COMMON/C/X(99,99),TIME(99,99),VEL(99,99),SS(99,99),PRESS(99,99),TE
  #MP(99,99),DENS(99,99),VELP(99,99),ENTR(99,99),VOLFRA(99,99),AL(99,
  ?99)
  COMMON/COM1/X3,X4,X6,T3,T4,T6,UG3,UG4,UG6,A3,A4,A6,PSI3,PSI4,PSI6,
  #TG3,TG4,TG6,RHO3,RHO4,RHC6,UP3,UP4,UP6,S3,S4,S6,EPL3,EPL4,EPL6,ARE
  >A3,AREA4,AREA6,L3,L4,L5,L6
  COMMON/CCM2/X12,T11,T12,T13,UG11,UG12,UG13,A11,A12,A13,PSI11,PSI12
  #,PSI13,TG11,TG12,TG13,RHC11,RHO12,RHO13,S11,S12,S13,EPL11,EPL12,EP
  #L13,AREA11,AREA12,AREA13,L11,L13,UP12
  COMMON/CCM3/X21,X22,X24,T21,T22,T24,UG21,UG22,UG24,A21,A22,A24,PSI
  #21,PSI22,PSI24,TG21,TG22,TG24,RHC21,RHO22,RHO24,S21,S22,S24,EPL21,
  #EPL22,EPL24,AREA21,AREA22,AREA24,L21,L24,NSTART
  COMMON/SAME/REGAS,PSI1,GAMMA,DZERC,PIE,BEE,PODPOT,CV,BASE,GZERO,WT,
  >TOL,AN
  COMMON/OUT/MAXJ,MAXI
  GO TO (10,11,12),LA
  10 WRITE(6,100)
  100 FORMAT(1H1,'EXCEEDED ITERATION LIMIT IN SUBROUTINE INTER')
  GO TO 15
  11 WRITE(6,101)
  101 FORMAT(1H1,'EXCEEDED ITERATION LIMIT IN SUBROUTINE BASE')
  GO TO 15
  12 WRITE(6,102)
  102 FORMAT(1H1,'EXCEEDED ITERATION LIMIT IN SUBROUTINE BREACH')
  15 WRITE(6,110)BUG,AA
  110 FORMAT(1H0,'LAST CALCULATED GAS VELOCITY',E12.3, '//2X, 'LAST CALCULA
  >TED SPEED OF SOUND',E12.3)
  105 FORMAT(1X,I3,1X,I3,E12.3,2X,E12.3,2X,E12.3,2X,E12.3,2X,E12.3,2X,E1
  #2.3,2X,E12.3,2X,F6.3)

```


SUBROUTINE START

C SUBROUTINE START

REAL L5,L6,L3,L4,L21,L24,L11,L13

COMMON/COM2/X12,T11,T12,T13,UG11,UG12,UG13,A11,A12,A13,PSI11,PSI12
#,PSI13,TG11,TG12,TG13,RHC11,RHO12,RHO13,S11,S12,S13,EPL11,EPL12,EP
#L13,AREA11,AREA12,AREA13,L11,L13,UP12COMMON/SAME/RGAS,PSI1,GAMMA,DZERC,PIE,BEE,PODPOT,CV,BASE,GZERO,WT,
#TOL,AN

COMMON/STAR/KSTART

AK=KSTART

ITRY=1

UG13=0.0

A13=A12

DELX=-0.125/AK

PSI13=PSI12

RHOP=3.1085

X13=X12+DELX

AREA12=TAREA(X12)

AREA13=TAREA(X13)

AREA=(AREA13+AREA12)/2.

Q12=2.*A12/(GAMMA-1.)

EPL13=EPL12

30 SLOPEQ=- (A13+A12)/2.

PSIMN=(PSI12+PSI13)/2.

T13=T12+(X13-X12)/SLOPEQ

BR13=BEE*((PSIMN/144.)*#AN)/12.

DL13=BR13*(T13-T12)

L13=L11+DL13

CALL DIME(L11,L13,SURF12,SURF13,VCL12,VOL13)

EPLMN=(EPL13+EPL12)/2.

VOLMN=(VOL13+VOL12)/2.

ETAMN=EPLMN/VOLMN

AMGMN=ETAMN*BR13*RHOP*AREA*(SURF13+SURF12)/2.

DEPLDT=-AMGMN/AREA/RHOP

TG13=A13+A13/GAMMA/RGAS

TGMN=(TG13+TG12)/2.

RHO13=PSI13/RGAS/TG13

RHOMN=(RHO13+RHO12)/2.

EGAS=PODPOT*AMGMN*GZERO

RS1=AMGMN*(CV+TGMN+PSIMN/778./RHCMN)+PSIMN*AREA*DEPLDT/778.

WORK=AREA*(1.-EPLMN)*RHOMN*TGMN

DSDT=(EGAS-RS1)/WORK

DELQDT=((A12+A13)/2.)*(778.*DSDT/RGAS+DEPLDT/(1.-EPLMN))

DELQDT=DELQDT+(((A12+A13)/2.)*#3)*AMGMN/AREA/PSIMN/(1.-EPLMN)/GAMM

#A

Q13=Q12+DELQDT*(T13-T12)

P13=Q13

ANEW13=(GAMMA-1.)*Q13/2.

TG13=ANEW13*ANEW13/GAMMA/RGAS

S13=S12+DSDT*778.*(T13-T12)/RGAS/GAMMA

PSI13=PSI12*((ANEW13/A12)**(2.*GAMMA/(GAMMA-1.)))

PSI13=PSI13*EXP(-GAMMA*(S13-S12))

RHO13=PSI13/RGAS/TG13

EPL13=EPL12+DEPLDT*(T13-T12)

CHECK=ABS((ANEW13-A13)/A13)

A13=ANEW13

IF(CHECK.GT.TOL) GO TO 180

X12=X13

RETURN

180 ITRY=ITRY+1

IF(ITRY.LT.11) GO TO 30

LOC=3

CALL DTAGO(LOC,UG13,A13)

RETURN
END

FUNCTION TAREA(ALOC)

C THIS IS A SUB PROGRAM TO CALCULATE THE BORE CROSS SECTIONAL AREA
DIMENSION BCRE(11),POS(11)

DATA BORE/0.024900,0.02491,0.02771,0.02746,0.02514,0.01864,0.018
>64,0.01824,0.01824,0.01824,0.01824/

DATA POS/- .10,0.0,0.02797,0.1032,0.1078,0.1135,0.1300,1.542,
\$3.0,5.0,15.0/

DO 10 I=1,11

IF(POS(I).EQ.ALOC) GO TO 5

IF(POS(I).GT.ALOC) GO TO 7

GO TO 10

5 TAREA=3.141593*BORE(I)*BCRE(I)*0.25

GO TO 15

7 AM=(BORE(I-1)-BORE(I))/(POS(I-1)-POS(I))

B=BORE(I)

DD=B+AM*(ALCC-POS(I))

TAREA=3.141593*DD*DD/4.

GO TO 15

10 CONTINUE

15 RETURN

END

SUBROUTINE DIME(A,B,SURA,SURB,VOLA,VOLB)

C SUBROUTINE DIME

C THIS IS A SUBROUTINE TO CALCULATE PROPELLANT SURFACE

C AREA AND VOLUME

DATA PIE,RBAR,RI/3.141593,0.00095,0.0006249/

WORK=RI-A

WORK1=RBAR-RI

VOLA=2.*PIE*WORK1*WORK1*WORK+PIE*PIE*WORK*WORK*(WORK1+
>4.*WORK/3./PIE)

SURA=2.*PIE*(PIE*WORK*(WORK1+2.*WORK/PIE)+WORK1*WORK1)

WORK=RI-B

VOLB=2.*PIE*WORK1*WORK1*WORK+PIE*PIE*WORK*WORK*(WORK1+
>4.*WORK/3./PIE)

SURB=2.*PIE*(PIE*WORK*(WORK1+2.*WORK/PIE)+WORK1*WORK1)

RETURN

END

SUBROUTINE INTER

C SUBROUTINE INTER

C THIS SUBROUTINE CALCULATES INTERIOR NETWORK POINTS

C

C

REAL L5,L6,L3,L4,L21,L24,L11,L13

COMMON/COM1/X3,X4,X6,T3,T4,T6,UG3,UG4,UG6,A3,A4,A6,PSI3,PSI4,PSI6,
>TG3,TG4,TG6,RHO3,RHO4,RHC6,UP3,UP4,UP6,S3,S4,S6,EPL3,EPL4,EPL6,ARE
>A3,AREA4,AREA6,L3,L4,L5,L6

COMMON/SAME/RGAS,PSI1,GAMMA,DZERC,PIE,BEE,PODPOT,CV,BASE,GZERO,WT,
>TOL,AN

COMMON/EXIT/XLIM,TMUZE

COMMON/BHEAT/FACT,TWALL,FRIC

COMMON/PARM/PARIN1,PARIN2,PARIN3,PARBA1,PARBA2,PARBA3,PARBR1,PARBR
\$2,PARBR3

DATA AMU,REC,RHOP/1.0445E-06,0.9,3.1085/

FUG=1.0

RI=SQRT(GAMMA*RGAS*530.)

1TRY=1

UG6=(UG3+UG4)/2.

A6=(A3+A4)/2.

TG6=(TG3+TG4)/2.

RHO6=(RHO3+RHO4)/2.

PSI6=(PSI3+PSI4)/2.

$UP6 = (UP3 + UP4) / 2.$
 $P3 = 2. * A3 / (GAMMA - 1.) + UG3$
 $Q4 = 2. * A4 / (GAMMA - 1.) - UG4$
 $EPL6 = (EPL3 + EPL4) / 2.$
 $AREA = (AREA3 + AREA4) / 2.$
 $S6 = (S3 + S4) / 2.$

C CALCULATION OF THE LOCATION OF THE NEW POINT ON X-T DIAGRAM

30 $SLOPEP = (UG3 + A3 + UG6 + A6) / 2.$
 $SLOPEQ = (UG4 - A4 + UG6 - A6) / 2.$
 $T6 = (X4 - X3 + T3 * SLOPEP - T4 * SLOPEQ) / (SLOPEP - SLOPEQ)$
IF (T6.GE.TMLZE) GO TO 25C
 $X6 = X3 + SLOPEP * (T6 - T3)$
31 $AREA6 = TAREA(X6)$
 $WORK = X4 - X3$
IF (T4.EQ.T3) GO TO 32
 $T7 = X6 - X3 + T3 * WORK / (T4 - T3) - T6 * UG6$
 $T7 = T7 / (WORK / (T4 - T3) - UG6)$
GO TO 33
32 $T7 = T3$
33 CONTINUE
 $X7 = X6 - UG6 * (T6 - T7)$
IF (T4.EQ.T3) GO TO 34
 $T5 = X6 - X3 + T3 * WORK / (T4 - T3) - T6 * UP6$
 $T5 = T5 / (WORK / (T4 - T3) - UP6)$
GO TO 35
34 $T5 = T3$
35 CONTINUE
 $X5 = X6 - UP6 * (T6 - T5)$
IF (X5.LT.0.0) X5=X3
 $WORK1 = (X7 - X3) / WORK$
 $UG7 = UG3 + (UG4 - UG3) * WORK1$
 $A7 = A3 + (A4 - A3) * WORK1$
 $S7 = S3 + (S4 - S3) * WORK1$
 $TG7 = A7 * A7 / (GAMMA * RGAS)$
 $WORK2 = 2. * GAMMA / (GAMMA - 1.)$
 $PSI7 = PSI3 * ((A7 / A3) ** WORK2)$
 $PSI7 = PSI7 * EXP(-GAMMA * (S7 - S3))$
 $RHO7 = PSI7 / RGAS / TG7$
 $WORK1 = (X5 - X3) / WORK$
 $UG5 = UG3 + (UG4 - UG3) * WORK1$
 $UP5 = UP3 + (UP4 - UP3) * WORK1$
 $A5 = A3 + (A4 - A3) * WORK1$
 $S5 = S3 + (S4 - S3) * WORK1$
 $TG5 = A5 * A5 / (GAMMA * RGAS)$
 $PSI5 = PSI3 * ((A5 / A3) ** WORK2)$
 $PSI5 = PSI5 * EXP(-GAMMA * (S5 - S3))$
 $RHO5 = PSI5 / RGAS / TG5$
 $EPL5 = EPL3 + (EPL4 - EPL3) * WORK1$
IF (EPL5.LE.0.00) EPL5=0.0
 $L5 = L3 + (L4 - L3) * WORK1$
 $UMN = (UG6 + UG7) / 2.$
 $UGMN = UMN$
 $AMN = (A6 + A7) / 2.$
 $TGMN = (TG6 + TG7) / 2.$
 $RHOMN = (RHO6 + RHO7) / 2.$
 $PSIMN = (PSI6 + PSI7) / 2.$
 $UP56 = (UP5 + UP6) / 2.$
 $RELV5 = ABS(UG5 - UP5)$
 $RELV6 = ABS(UG6 - UP6)$
 $RELV56 = (RELV5 + RELV6) / 2.$
 $PEE56 = (PSI5 + PSI6) / 2.$
 $BR56 = BEE * ((PEE56 / 144.) ** AN) / 12.$
IF (RELV56.GT.500.) BR56=BR56*(1.+C.0004*(RELV56-500.))

```

DL56=BR56*(T6-T5)
L6=L5+DL56
IF(L5.GT.0.C00625)L5=0.CC0625
IF(L6.GT.0.C00625)L6=0.CC0625
CALL DIME(L5,L6,SURF5,SURF6,VCL5,VCL6)
IF(VOL5.LE.0.00)SURF5=0.C0
IF(VOL6.LE.0.00)SURF6=C.00
EPL56=(EPL6+EPL5)/2.
DBAR=DZERO-L5-L6
IF(DBAR.LT.0.C00652)DBAR=0.00
REY56=RELV56*DBAR/AMU
REY56=REY56*(RHO5+RHO6)/2.
IF(REY56.LE.0.000) GO TO 98
CDRAG=28./(REY56**(0.85))+0.48
GO TO 99
98 CDRAG=0.0
GO TO 99

```

C CALCULATION OF VELOCITY AND PRESSURE GRADIENTS

```

99 IF(T3.GT.T4) GO TO 100
T8=T4
X8=(UG3+A3)*(T8-T3)+X3
PSI8=PSI3+(PSI6-PSI3)*(X8-X3)/(T6-X3)
UP8=UP3+(UP6-UP3)*(X8-X3)/(X6-X3)
DPDX=0.00
DUPDX=(UP4-UP8)/(X4-X8)
GO TO 125
100 T8=T3
X8=(UG4-A4)*(T8-T4)+X4
PSI8=PSI4+(PSI6-PSI4)*(X4-X8)/(X4-X6)
UP8=UP4+(UP6-UP4)*(X4-X8)/(X4-X6)
DPDX=0.00
DUPDX=(UP8-UP3)/(X8-X3)

```

125 CONTINUE

C DRAG FORCE ON PROPELLANT PARTICLE

```

FOR56=CDRAG*(RHO5+RHO6)*RELV56*RELV56
FOR56=FOR56*DBAR*DBAR/16.
FOR56=FOR56-DPDX*(DBAR**3)/6.
FOR56=FOR56*PIE
IF(VOL5.LE.C.00.AND.VCL6.LE.0.00)GO TO 1125
ETA56=2.*EPL56/(VOL5+VCL6)
GO TO 1126
1125 ETA56=0.00
1126 CONTINUE

```

FD56=ETA56*FOR56

C MASS OF GAS GENERATED GOING FROM 5 TO 6

```

AMG56=ETA56*BR56*RHOP*AREA
AMG56=AMG56*(SURF5+SURF6)/2.
AMG56=AMG56*FUG

```

C CHANGE IN PARTICLE VELOCITY AND MASS FRACTION

```

IF(EPL56.LE.0.000) GO TO 126
DUPDT =UP56*AMG56/RHOP/AREA/EPL56
DUPDT=DUPDT+FD56/RHOP/EPL56
GO TO 127
126 DUPDT=0.00
127 CONTINUE
DEPLDT=-EPL56*DUPDT/UP56
DEPLDT=DEPLDT-AMG56/RHOP/AREA
DIA=SQRT(4.*AREA/PIE)
FILM=FRICT*GAMMA*RGAS*RHCMN*UGMN/2./(GAMMA-1.)/778.
TAW=TGMN*(1.+REC*(GAMMA-1.)*UGMN*UGMN/2./AMN/AMN)
QHEAT=FILM*(TAW-TWALL)
QHEAT=QHEAT*FACT
EGAS=-QHEAT*PIE*DIA-FD56*AREA*RELV56/778.

```

```

LONJ-EGM37AFU30+PUUPUI*GZERU
TAUW=0.5*FRICT*RHOMN*UGMN*UGMN
F1= UGMN*AMG56+TAUW*PIE*DIA+FD56*AREA
F1=F1/778.
RS1=AMG56*(CV*TGMN+UGMN*UGMN/1556.)*PSIMN*AREA*DEPLDT/778.
RS1=RS1+PSIMN*AMG56/RHCMN/778.
WORK=AREA*(1.-EPL56)*RHOMN*TGMN
DSDT=AMG56*(PODPOT*GZERO-(CV+RGAS/778.)*TGMN)+FD56*AREA*(UGMN-RELV
#56)/778. +(TAUW*UGMN/778.-GHEAT)*PIE*DIA -PSIMN*AREA*DEPLDT/778.
DSDT=DSDT/WCRK
IF(T6.GE.PARIN1) GO TO 201
128 CONTINUE
C CALCULATE THE CHANGE IN P AND C
UG36=(UG3+UG6)/2.
RHO36=(RHO3+RHO6)/2.
PSI36=(PSI3+PSI6)/2.
AREA=(AREA3+AREA6)/2.
A36=(A3+A6)/2.
EPL36=(EPL3+EPL6)/2.
TRY=A36*A36*778.*(S6-S3)/(X6-X3)/GAMMA/RGAS
DELPDT=-A36*UG36*(AREA3-AREA6)/(X3-X6)/AREA
DELPDT=DELPDT+A36*778.*DSDT/RGAS
WORK=TAUW*PIE*DIA/AREA/(1.-EPL36)/RHO36
WORK=WORK+FC56/RHO36/(1.-EPL36)
DELPCT=DELPDT-WORK
DELPDT=DELPCT+A36*DEPLCT/(1.-EPL36)+((A36**3)/PSI36/GAMMA-UG36/RHO
>36)*AMG56/AREA/(1.-EPL36)
DELPCT=DELPCT+TRY
PSI46=(PSI4+PSI6)/2.
EPL46=(EPL4+EPL6)/2.
A46=(A4+A6)/2.
UG46=(UG4+UG6)/2.
RHO46=(RHO4+RHO6)/2.
AREA=(AREA4+AREA6)/2.
TRY=A46*A46*778.*(S6-S4)/(X6-X4)/GAMMA/RGAS
DELDQT=-A46*UG46*(AREA4-AREA6)/(X4-X6)/ARE/
DELDQT=DELDQT+A46*778.*DSDT/RGAS
WORK=(TAUW*PIE*DIA/AREA+FD56)/(1.-EPL46)/RHO46
DELDQT=DELDQT+WORK+A46*DEPLCT/(1.-EPL46)
DELDQT=DELDQT+((A46**3)/PSI46/GAMMA+UG46/RHO46)*AMG56/AREA/(1.-EPL
#46)
DELDQT=DELDQT-TRY
P6=P3+DELPDT*(T6-T3)
Q6=Q4+DELDQT*(T6-T4)
ANEW6=(GAMMA-1.)*(P6+Q6)/4.
UGNEW6=(P6-Q6)/2.
S6=S7+DSDT*(T6-T7)*778./RGAS/GAMMA
EPL6=EPL5+DEPLDT*(T6-T5)
IF(EPL6.LE.0.00)EPL6=0.0
UPN6=UP5+DUPDT*(T6-T5)
IF(EPL6.LE.0.00)UPN6=LGNEW6
TG6=ANEW6*ANEW6/GAMMA/RGAS
PSI6=PSI7*!(ANEW6/A)*WCRK2)
PSI6=PSI6*EXP(-GAMMA*(S6-S7))
RHO6=PSI6/RGAS/TG6
IF(T6.GE.TMLZE) GO TO 260
5003 FORMAT(1X,5E11.3)
CHECK=ABS((ANEW6-A6)/A6)
IF(CHECK.GT.TOL) GO TO 180
CHECK=ABS((LGNEW6-UG6)/UG6)
IF(UG6.(T.300.) CHECK=0.C0001
TOLL=10.*TCL
IF(CHECK.GT.TOLL) GO TO 180

```

```

UOLD4=UG4
AOLD4=A4
XOLD4=X4
SOLD4=S4
PSIOL4=PSI4
UPOLD4=UP4
XOLD4=X4
RETURN
180 ITRY=ITRY+1
IF(ITRY.LT.21) GO TO 200
LOC=1
CALL DIAGQ(LOC,UGNEW6,ANEW6)
200 UG6=(UGNEW6+UG6)/2.
A6=(ANEW6+A6)/2.
UP6=(UPN6+UP6)/2.
GO TO 30
201 WRITE(6,5004)VOL5,VOL6,SLRF5,SURF6,ETA56,ANG56,EPL56,DUPDT,DEPLDT
WRITE(6,5004)L5,L6,X5,X6,BR56
WRITE(6,5004)P6,Q6,A6,LG6,UP6
DVOL=2.*((3.*VOL5/(4.*FIE))*0.33)
WRITE(6,5004)FD56,TAUW,EGAS,RS1,F1,UGMN,FOR56,UP3,UP4,UP5,DUPDX,UP
#56,UG5,DBAR,DVOL,UPN6
5004 FORMAT(1X,5E20.5)
GO TO 128
250 T6=TMUZE
X6=X3+SLOPEP*(T6-T3)
AQ=(UG3+UOLC4-A3-AOLD4)/2.
AP=(UOLD4+UG4+A4+AOLD4)/2.
TI=(X4-X6+AQ*T6-AP*T4)/(AQ-AP)
XI=X4+AP*(TI-T4)
UG4=(UG4-UOLD4)*(XI-X4)/(XCLD4-X4)+UG4
A4=(A4-AOLD4)*(XI-X4)/(XOLD4-X4)+A4
TG4=A4*A4/GAMMA/RGAS
PSI4=(PSI4-PSIOL4)*(XI-X4)/(XOLD4-X4)+PSI4
RHO4=PSI4/RGAS/TG4
UP4=(UP4-UPCLD4)*(XI-X4)/(XCLD4-X4)+UP4
S4=(S4-SOLD4)*(XI-X4)/(XCLC4-X4)+S4
X4=XI
T4=TI
GO TO 31
260 UG6=UGNEW6
A6=ANEW6
UP6=UPN6
RETURN
END

```

APPENDIX B
Listing of Flame Front Program

```
/PROGRAM MCASSEY
C PROGRAM CALCULATES THE PROPAGATION OF A FLAMEFRONT THRU A
C POROUS PROPELLANT BED
C F=PROPELLANT IMPETUS (FT-LBS/LB)
C C= CHARGE WT (LBS)
C RHOP= PROPELLANT DENSITY (LBS/IN**3)
C ALFA=FLAMEFRONT VELOCITY PRESSURE COEFFICIENT (IN/SEC-PSI**BETA)
C BEYA=FLAMEFRONT VELOCITY PRESSURE EXPONENT (DIMEN)
C B=PROPELLANT BURNING RATE COEFFICIENT (IN/(SEC-PSI**EN))
C EN=PROPELLANT BURNING RATE EXPONENT (DIMEN)
C R0=EQUIV. MEAN RADIUS OF PROP. GRAIN (IN)
C RI=1/2 WEB THIN)
C XLO=LENGTH OF COMPACTION REGION (IN)
C ETA=PROPELLANT COVOLUME (IN**3/LB)
1 DIMENSION P(30),PBAR(30),VF(30),DL(30),XL(30,30),RL(30,33),V(30,30
$),XMG(30,30),ZL(30),CL(30),E(30,30)
C SUBSCRIPT J DENOTES THE NUMBER OF TIME INTERVALS (PT) DURING WHICH
C THE FLAMEFRONT PENETRATES THE PROPELLANT, J=1 CORRESPONDE TO IGNITIO
2 DATA RHOP, R0, RI, XLO, ETA/0.0567, 0.0115, 0.0075, 0.23, 32.2/
3 2 READ(5, 5000) F, ALFA, BETA, B, EN, FACT
4 READ(5, 5000) RGAS, GAMMA, CV, TZERO
5 5000 FORMAT(2E20.5)
6 WRITE(6, 5000) F, ALFA, BETA, B, EN, FACT
7 WRITE(6, 5000) RGAS, GAMMA, CV, TZERO
8 VEL=0.0
9 AZERO=SQRT(GAMMA*RGAS*TZERO)
10 C=4.014E-03
11 ICOUNT=0
12 DO 10 I=1, 30
13 DO 10 J=1, 30
14 F(I, J)=0.0
15 10 XL(I, J)=0.0
16 PIE=3.1415
17 T=0.0001
18 XTG=0.0
19 RR=R0-RI
20 V0I=2.*PIE*RR*RR*RI+PIE*PIE*RI*RI*(RR+1.333*RI/PIE)
C XN=THE NUMBER OF GRAINS PER UNIT VOLUME
C A=CROSS SECTIONAL AREA OF CARTRIDGE
C D=DIAMETER OF CARTRIDGE CASE 0.335
21 A=PIE*0.335*0.335/4.
C VC=VOLUME OCCUPIED BY COMPRESSED PROPELLANT
22 VC=A*(1.5-XLO)
23 XN=C/(RHOP*V0I*VC)
24 WRITE(6, 1234)
25 P(1)=2750.
26 DO 1000 J=2, 29
27 P(J)=P(J-1)
28 DT=0.25E-04
29 T=T+DT
30 801 ICOUNT=ICOUNT+1
C SUBSCRIPT J DENOTES THE NUMBER OF TIME INTERVAL (DT) DURING WHICH
C THE FLAMEFRONT PENETRATES THE PROPELLANT BED (IGNIT TIME=0.0001S)
C
C CALCULATE THE DISTANCE (D(J)) THE FLAMEFRONT HAS TRAVELED
31 PBAR(J)=(P(J-1)+P(J))/2.
32 VF(J)=ALFA*PBAR(J)**BETA
33 DL(J)=VF(J)*DT
34 ZL(1)=XLO
CL(1)=XLO
```

```

37 IF(ZL(J).GE.1.5) ZL(J)=1.5
38 IF(ZL(J).GE.1.5)DL(J)=ZL(J)-ZL(J-1)
39 IF(ZL(J).GE.1.5)T=T-DT
40 IF(ZL(J).GE.1.5)DT=DL(J)/VF(J)
41 IF(ZL(J).GE.1.5)T=T+DT

C
C CALCULATE THE DISTANCE(XL(I,J)) BURNED NORMAL TO PROP. SURFACE(IN)
C CELL I DURING TIME DT, I=1 IS INITIAL COMPACTION REGION(NO PROP.)
42 PXTG=0.0
43 VOL5=0.0
44 DO 500 I=2,J
45 DXL=B*PBAR(J)**EN*DT
46 DXL=DXL*FACT
47 XL(I,J)=XL(I,J-1)+DXL
48 RL(I,J)=RI-XL(I,J)
49 V(I,J)=2.*PIE*(RR**2*RL(I,J))+PIE*PIE*RL(I,J)**2*(RR+1.333/PIE*RL(
#I,J))

C
C XMG(I,J) IS THE AMOUNT OF GAS GENERATED FROM CELL I DURING TIME T
50 XMG(I,J)=DL(I)*XN*A*(VOI-V(I,J))*RHOP
C XTG=THE TOTAL GAS GENERATED IN TIME T
51 DXMG=XMG(I,J)
52 E(I,J)=(XN*A*DL(I)*VOI-XMG(I,J)/RHOP)/A/DL(I)
53 VOL5=VOL5+A*DL(I)*E(I,J)
54 PXTG=PXTG+DXMG
55 500 CONTINUE
56 XNUM=12.*PXTG*F+P(1)*A*ZL(1)
57 DENOM=A*ZL(J)-VOL5-PXTG*ETA
58 PPBAR=XNUM/DENOM
59 IMN=J
60 IF(ABS((PPBAR-P(J))/PPBAR)-0.05)55,55,800
61 800 IF(ICOUNT.GT.25) GO TO 1001
62 P(J)=PPBAR
63 GO TO 801
64 55 CONTINUE
65 XTG=PXTG
66 P(J)=PPBAR
67 ICOUNT=0
68 DO 900 I=2,J
69 WRITE(6,2468)T,P(J),ZL(J),XTG,F(I,J),XL(I,J),I,J
70 TIME=T
71 900 CONTINUE
72 IF(ZL(J).GE.1.5) GO TO 1001
73 K=J
74 CL(J)=ZL(J)
75 1234 FORMAT(1H1,9X,'TIME',15X,'HP(J)',15X,'ZL(J)',15X,'XTG',15X,'E(I,J)
#')
76 2468 FORMAT(6(4X,E15.6),2I3)
77 1000 CONTINUE
78 DO 1002 J=2,9
79 DO 1002 I=2,9
80 WRITE(6,2468)XL(I,J),DXL,V(I,J),XMG(I,J),RL(I,J),DL(I),I,J
81 1002 CONTINUE
82 GO TO 1005
83 1001 CONTINUE
84 J=IMN
85 P(J)=P(J)*144.
86 DEN5=P(1)/RGAS/TZERO
87 FNTR=(RGAS/778.*CV)*ALOG(TZERO/530.)-RGAS/778.*ALOG(P(J)/2075.)
88 FNTR=FNTR*778./RGAS/GAMMA
89 DO 1004 I=1,IMN
90 DIST=ZL(I)/12.
91 XL(I,J)=XL(I,J)/12.

```

```
92      TIM=T+(0.125-DIST)/AZERO
93      WRITE(7,4445)I,J
94      WRITE(7,4444)DIST,TIM,E(I,J),AZERO,VFL,VEL,P(J),DENS,ENTR,XL(I,J)
      $,TZERO
95      WRITE(6,4444)DIST,TIM,E(I,J),AZERO,VFL,VEL,P(J),DENS,ENTR,XL(I,J)
      $,TZERO
96      WRITE(7,4445)I,J
97      1004 CONTINUE
98      4445 FORMAT(5X,'*****',5X,I4,5X,I4,5X,'*****'5X)
99      4444 FORMAT(3E20.5)
100     1005 CONTINUE
101     GO TO 2
102     END
```

/G)

0.32060E 06	0.31500E 02
0.48000E 00	0.26300E-02
0.70000E 00	0.10000E 01
0.25643E 04	0.12506E 01
0.11470E 02	0.46150E 04